Design, synthesis, in-vitro antiproliferative activity and kinase profile of new picolinamide based 2-amido and ureido quinoline derivatives

ARTICLE *in* EUROPEAN JOURNAL OF MEDICINAL CHEMISTRY · JULY 2015

Impact Factor: 3.45 · DOI: 10.1016/j.ejmech.2015.07.025 · Source: PubMed

7 AUTHORS, INCLUDING:

Ashraf Kareem

Korea University of Science and Technology

3 PUBLICATIONS **1** CITATION

SEE PROFILE

Nam-chul Cho

Korea Institute of Science and Technology

17 PUBLICATIONS **26** CITATIONS

SEE PROFILE

soon-bang Kang

Korea Institute of Science and Technology

55 PUBLICATIONS **547** CITATIONS

SEE PROFILE

Gyochang Keum

Korea Institute of Science and Technology

71 PUBLICATIONS **580** CITATIONS

SEE PROFILE

European Journal of Medicinal Chemistry 101 (2015) 754–768

Contents lists available at ScienceDirect

European Journal of Medicinal Chemistry

journal homepage: http://www.elsevier.com/locate/ejmech

Research paper

Design, synthesis, *in-vitro* antiproliferative activity and kinase profile of new picolinamide based 2-amido and ureido quinoline derivatives

Ashraf Kareem El-Damasy [a, b, c], Seon Hee Seo [a], Nam-Chul Cho [a, d], Soon Bang Kang [a], Ae Nim Pae [a, b], Key-Sun Kim [a], Gyochang Keum [a, b, *]

[a] Center for Neuro-Medicine, Brain Science Institute, Korea Institute of Science and Technology (KIST), Hwarangro 14-gil 5, Seongbuk-gu, Seoul 136-791, Republic of Korea
[b] Department of Biological Chemistry, Korea University of Science and Technology (UST), Gajungro 217, Youseong-gu, Daejeon 305-350, Republic of Korea
[c] Department of Medicinal Chemistry, Faculty of Pharmacy, University of Mansoura, Mansoura 35516, Egypt
[d] Department of Biotechnology, Yonsei University 220, Seoul 120-749, Republic of Korea

ARTICLE INFO

Article history:
Received 22 May 2015
Received in revised form
14 July 2015
Accepted 15 July 2015
Available online 17 July 2015

Keywords:
Antiproliferative activity
Quinoline
Urea
Amide
Picolinamide
$BRAF^{V600E}$
C-RAF

ABSTRACT

New 2-amido and ureido quinoline derivatives substituted with 2-*N*-methylamido-pyridin-4-yloxy group at the 5-position of quinoline (18 final compounds) have been designed and synthesized as anticancer sorafenib congeners. Among the synthesized derivatives, fourteen compounds were selected for evaluation of their antiproliferative activity over a panel of 60 cancer cell lines at a single dose concentration of 10 μM at National Cancer Institute (NCI, USA). Four compounds, **9b**–**d** and **9f** showed promising mean growth inhibitions and thus were further tested at five-dose testing mode to determine their IC_{50} values. The data revealed that 2,4-difluorophenyl (**9b**) and 4-chloro-3-trifluoromethylphenyl (**9d**) urea compounds are the most active derivatives with significant efficacies and superior potencies than sorafenib in 36 and 12 cancer cell lines, respectively, belonging particularly to renal carcinoma cell (RCC), ovarian, and non small cell lung cancer (NSCL). Compound **9b** and **9d** were found to be six and two times more potent than sorafenib against A498 RCC line, with IC_{50} values of 0.42 μM and 1.36 μM, respectively. Accordingly, compound **9d** was screened over a panel of 41 oncogenic kinases at a single dose concentration of 10 μM to profile its kinase inhibitory activity. Interestingly, the compound showed highly selective inhibitory activities (81.8% and 96.3%) against $BRAF^{V600E}$ and C-RAF kinases with IC_{50} values of 316 nM and 61 nM, respectively. In addition, molecular docking, cell cycle analysis, compliance to Lipinski's rule of five, and *in silico* toxicity assessment have been reported.

1. Introduction

In spite of the immense research endeavors and profound advances in cancer detection and treatment, cancer is still one of the most challenging health problems worldwide, being the second common cause of death after cardiovascular diseases [1]. As stated by the World Health Organization (WHO), the number of new cases is expected to increase by about 70% over the next 2 decades [2]. The current available treatments for most types of cancer, such as chemotherapeutic agents and radiotherapy provide only temporal therapeutic benefits as well as being limited by a narrow therapeutic index, remarkable toxicities and often acquired resistance [3]. Therefore, there is a growing imperative need for further identification and development of new treatment approaches, especially the discovery of new chemotherapeutics with improved potency and minimal side effects.

Among the plethora of compounds evaluated as potential antiproliferative agents, derivatives possessing the *N*-methyl picolinamide, diarylurea and/or diarylamide structural features have attracted great attention of contemporary medicinal chemists [4–9]. Sorafenib (Nexavar®, **A** in Fig. 1), for example, is a diarylurea anticancer agent that was originally developed to target C-RAF (RAF1) kinase [10]. Nevertheless, the structural motifs of sorafenib displayed multiple kinase inhibitory effects with potent antitumorigenic and antiangiogenic activities through the inhibition of several receptor tyrosine kinases (RTKs), like the VEGFR-2 and VEGFR-3 [11], FLT3 and c-KIT [12–14]. Nowadays, sorafenib is used

* Corresponding author. Center for Neuro-Medicine, Brain Science Institute, Korea Institute of Science and Technology (KIST), Hwarangro 14-gil 5, Seongbuk-gu, Seoul 136-791, Republic of Korea.
E-mail address: gkeum@kist.re.kr (G. Keum).

http://dx.doi.org/10.1016/j.ejmech.2015.07.025
0223-5234/

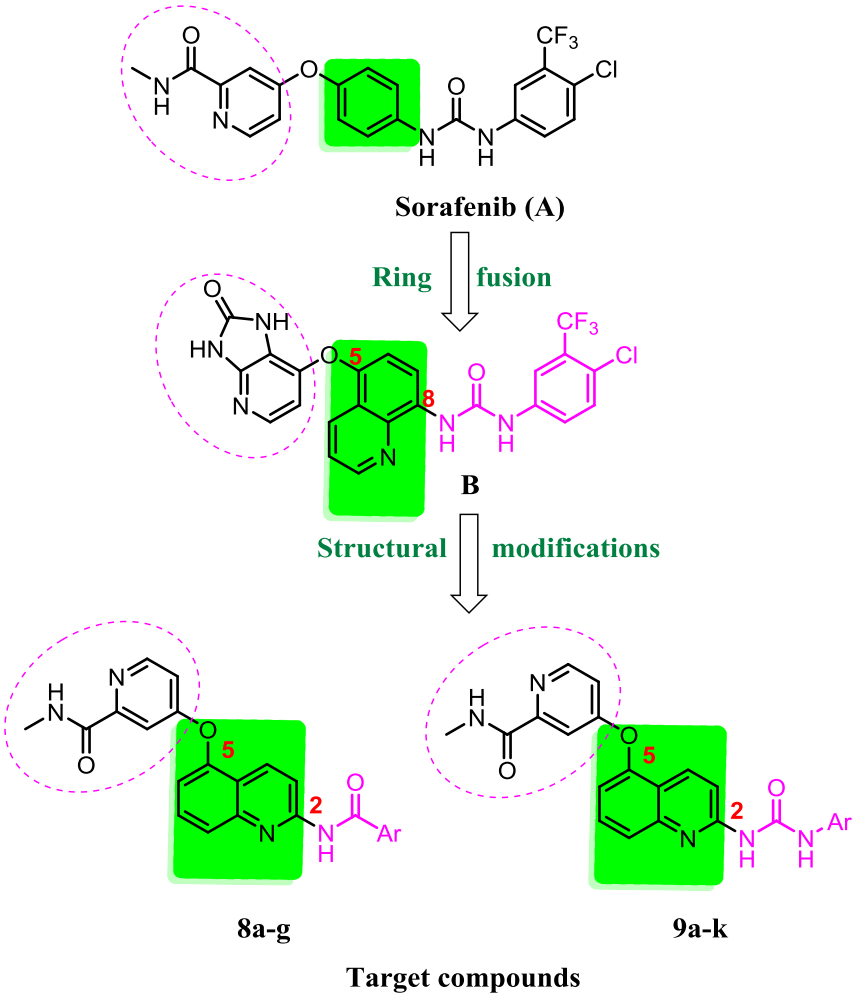

Fig. 1. Sorafenib (**A**), its quinoline congener (**B**) and the designed compounds.

for the treatment of hepatocellular carcinoma (HCC) [15,16] and renal cell carcinoma (RCC) [13,17], in addition to being currently in clinical trials for combating other tumor types such as neuroblastoma and leukemia [18]. Despite of the diverse merits of sorafenib, such as multi-mechanisms and broad-spectrum antitumor activity, still it possesses some drawbacks of poor physicochemical properties [19], scanty therapeutic activity in the treatment of malignant melanoma [20], and accompanying toxicities [21–23]. Therefore, more and more attentions have paid for further optimization of sorafenib [19,24–28].

Among these efforts, Ion et al. [29] changed the central phenyl ring of sorafenib with quinoline, together with replacing the *N*-methyl picolinamide tail of sorafenib with 2-oxo-2,3-dihydro-1*H*-imidazo[4,5-b]pyridine (Fig. 1). Such structural modifications, exemplified by compound **B**, led to significant improvement of both cellular and enzymatic activity of sorafenib over RAF kinases and their correlated cancer cells, yet showing lack of selectivity among the other protein kinases (multikinase inhibitors) with potential concomitant toxicity.

Inspired by the promising activity of previously described derivatives, two new series of *N*-methylpicolinamide based 2,5-disubstituted quinolines were designed and synthesized. Our design approach was relied on introducing 2-*N*-methylamidopyridin-4-yloxy group in the 5-position of quinoline, conserving picolinamide group of sorafenib, and the arylurea moiety at C-2 position of quinoline (Fig. 1). Moreover, we explored the amide spacer to study its effect on the antiproliferative activity in comparison to urea linker. The target compounds, **8a**–**g** and **9a**–**k** were evaluated for their *in vitro* antiproliferative activities against 60 human cancer cell lines representing 9 different tumor types, and the kinase inhibitory profile for one of the most potent derivatives, compound **9d** was also examined to investigate the mechanism of action at molecular level.

2. Results and discussion

2.1. Chemistry

The synthetic route for preparation of the key starting material, 2-amino-5-quinolinol (**6**), not reported so far, is illustrated in Scheme 1. Methylation of the commercially available 5-hydoxyquinoline, *via* Williamson ether synthesis, was reported to proceed using diazomethyltrimethyl silane with 42% yield [30,31]. Herein, we optimized such reaction by adopting sodium hydride induced deprotonation of the hydroxy compound in anhydrous *N*,*N*-dimethylformamide (DMF) under argon atmosphere, followed by dropwise addition of methyl iodide and stirring for 30 min at room temperature to afford the corresponding methoxy derivative

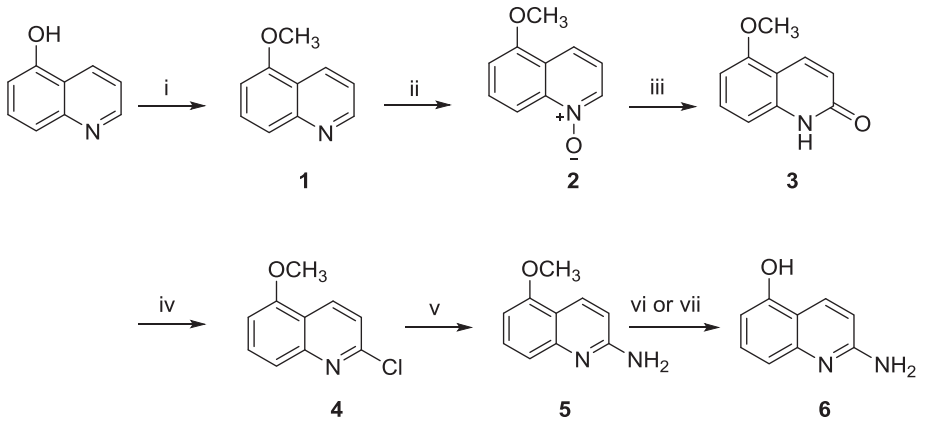

Scheme 1. Reagents and reaction conditions: i) NaH, DMF, 0 °C, 30 min, CH_3I, 0 °C to rt, 30 min, 92%; ii) *m*CPBA, DCM, 0 °C to rt, 6 h, 92%; iii) TsCl, 10% aq. K_2CO_3, DCM, rt, 18 h, 65%; iv) $POCl_3$, reflux, 1 h, 86%; v) Acetamide, K_2CO_3, neat, 200 °C, 15 h, 47%; vi) BBr_3, DCM, 0 °C to rt, 18 h, 51%; vii) 48% HBr, reflux, 8 h, 88%.

1 in excellent yield (92%). Compound **1** was then *N*-oxidized with *m*-chloroperoxybenzoic acid (*m*-CPBA) to provide 5-methoxyquinoline-*N*-oxide (**2**) [30,31]. The direct conversion of the *N*-oxide **2** to the corresponding 2-chloro derivative **4** was reported to occur, yet with low yield (32%) [30,31]. Therefore, we followed another synthetic approach, based on treatment of the *N*-oxide **2** with *p*-tosyl chloride in 10% aqueous potassium carbonate (K_2CO_3)/dichloromethane (DCM) system to produce the reactive lactam form of quinoline **3**, which then smoothly chlorinated with excess phosphorous oxychloride furnishing the 2-chloro-5-methoxyquinoline (**4**) in good yield (86%). Fusion of the chloro compound **4** with excess acetamide in the presence of K_2CO_3 at elevated temperature (200 °C) for 15 h afforded the corresponding amino derivative **5** in moderate yield (47%). Refluxing of the methoxyquinoline **5** in 48% aqueous hydrobromic acid, or treatment with boron tribromide (BBr_3) in DCM at 0 °C afforded the demethylated derivative **6** in 88% and 51% yield, respectively. Herein, we developed a straightforward facile method for the synthesis of compound **6** with simple work-up procedure, utilizing compounds **1**–**4** in their crude forms which were of high purity, as indicated by ^{1}H NMR spectra.

As shown in Scheme 2, all of the final compounds **8a**–**g** and **9a**–**k** were synthesized utilizing the novel intermediate, 5-oxypicolinamide quinoline-2-yl amine (**7**). It was obtained, in good yield (74%), by selective *O*-arylation of compound **6** with 4-chloro-*N*-methyl picolinamide using cesium carbonate as a base in DMSO at 135 °C. The selective installation of picolinamide moiety at the hydroxyl group of **6** was confirmed by existence of NH_2 proton in ^{1}H NMR spectra of **7**. Condensation of the amine compound **7** with the appropriate aryl carboxylic acids in the presence of *O*-(7-azabenzotriazol-1-yl)-*N*,*N*,*N*′,*N*′-tetramethyluronium hexafluorophosphate (HATU) and the Hünig's base (diisopropylethylamine, DIPEA) in anhydrous DMF afforded the corresponding amide derivatives **8a**–**g**. On the other hand, the synthesis of urea compounds **9a**–**k** was accomplished by treating the amine intermediate **7** with the proper aryl isocyanates in anhydrous DCM under argon atmosphere.

2.2. In vitro screening of the antiproliferative activities

2.2.1. Preliminary evaluation against 3 human cancer cell lines

All final compounds were preliminary evaluated for their antiproliferative activity at two concentrations of 100 and 10 μM against three cancer cell lines, MCF-7 and SK-BR3 (breast cancer cells) and HCT-116 (human colorectal carcinoma) by MTT assay method and sorafenib was used as the reference compound. The percentages growth inhibition (GI) of the tested compounds against the three cell lines are illustrated in Table 1. The results revealed the modest cytostatic activity of all amide spacer containing derivatives, except compound **8d**. In contrast, most of the investigated urea compounds showed promising and comparable (marginally superior or inferior) antiproliferative activity to that of

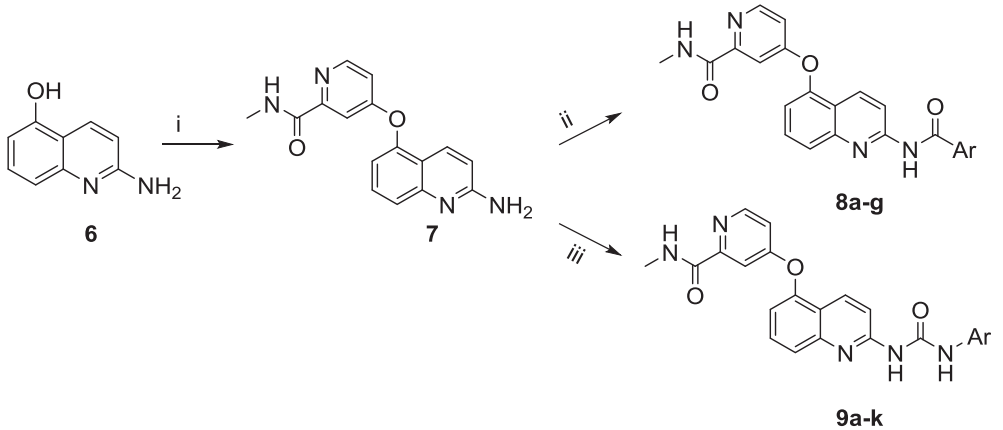

Scheme 2. Reagents and reaction conditions: i) 4-Chloro-*N*-methyl picolinamide, Cs_2CO_3, DMSO, 135 °C, 5 h, 74%; ii) $ArCO_2H$, HATU, DIPEA, DMF, rt, 24 h, 23–92%; **8g**, 80 °C, 5 h, 36% iii) Aryl isocyanate, DCM, 0 °C to rt, 24 h, 46–100%.

Table 1
Preliminary antiproliferative activity of the target compounds against a panel of 3 human cancer cell lines.

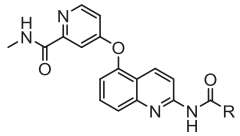

Compound no.	R	% Growth inhibition[a]					
		HCT-116		MCF-7		SK-BR-3	
		100 μM	10 μM	100 μM	10 μM	100 μM	10 μM
8a	2,4-Cl_2–C_6H_3–	61.64	15.63	44.32	12.24	60.45	9.49
8b	3,5-Cl_2–C_6H_3–	1.90	−2.80	39.16	6.30	17.04	4.22
8c	3,5-$(CF_3)_2$–C_6H_3–	62.04	15.75	48.82	16.75	57.94	14.83
8d	4-Cl-3-CF_3–C_6H_3–	77.51	55.45	56.55	42.42	65.43	26.31
8e	6-Cl-pyridin-2-yl	64.57	37.29	32.51	15.20	53.31	30.40
8f	Quinolin-6-yl	71.77	58.21	38.72	34.73	68.16	40.56
8g	1,4-Benodioxan-6-yl	48.40	1.73	36.33	10.09	49.90	1.90
9a	2,4-Cl_2–C_6H_3–NH	87.73	64.21	69.25	37.54	80.47	34.71
9b	2,4-F_2–C_6H_3–NH	89.49	60.03	NT[b]	NT[b]	93.41	82.22
9c	3,5-$(CF_3)_2$–C_6H_3–NH	91.59	57.28	64.49	38.72	91.68	63.14
9d	4-Cl-3-CF3–C6H3–NH	90.89	74.67	66.52	43.62	81.01	59.34
9e	2-Cl–5-CF_3–C_6H_3–NH	79.14	58.21	NT[b]	NT[b]	83.52	73.52
9f	3,4-Cl_2–C_6H_3–NH	76.93	60.18	48.05	27.05	59.21	36.86
9g	4-Cl–C_6H_4–NH	62.65	52.45	31.53	13.17	40.96	11.13
9h	4-Br–C_6H_4–NH	17.69	8.27	47.25	25.76	37.60	25.57
9i	4-F–C_6H_4–NH	64.30	60.29	38.46	23.51	46.50	25.19
9j	4-CF_3–C_6H_4–NH	75.96	63.12	NT[b]	NT[b]	75.73	53.63
9k	1-Naphthyl–NH	91.96	68.27	78.36	35.56	94.50	29.36
Sorafenib		97.32	48.41	96.06	40.45	93.12	48.87

[a] Compounds were tested in duplicate mode at concentrations of 100 and 10 μM.
[b] NT, not tested.

sorafenib, particularly against both HCT-116 and SK-BR3 cancer cell lines.

2.2.2. *In vitro antiproliferative activities against NCI-60 cell line panel*

2.2.2.1. Single dose testing. Encouraged by the favorable preliminary anticancer activity and in order to broadly explore the antiproliferative activity of the synthesized compounds, their structures were submitted to National Cancer Institute (NCI, Bethesda, Maryland, USA) [32], and 14 compounds out of 18 were selected on the basis of degree of structural variation and computer modeling techniques for assessment of their antiproliferative activity. The selected compounds were prescreened according to the NCI protocol at a single dose concentration of 10 μM on the full panel of approximately 60 human cancer cell lines derived from 9 human cancer cell types including; leukemia, non-small cell lung, colon, central nervous system, melanoma, ovarian, renal, prostate, and breast tumor cell lines. The mean percentages GI of the tested compounds over the full panel of cell lines are illustrated in Fig. 2.

As revealed from the results, all amide spacer containing derivatives, **8a**, and **8c**–**g**, possess weak anticancer activity (mean % GI = −3.16 to 11.08) even with variation of substituents at the terminal aryl moiety. On the other hand, it was found that the urea derivatives **9c** and **9d** were more potent (mean % GI = 69.95 and 80.32, respectively) than the corresponding amides **8c** and **8d** (mean % GI = 2.69 and −3.16, respectively), which indicates the indispensable nature of urea as spacer for the anticancer activity. This may be owed to that the longer linker, urea moiety, may geometrically warrant favorable fitting of the molecule at the active site. Or the terminal NH group of the urea moiety may form additional hydrogen bond(s) at the receptor site. Any or both of these effects would enable optimal drug interaction in the enzyme active site, and hence higher anticancer activity.

Moreover, the effects of substitution pattern (nature and position) of the terminal phenyl ring on the activity of urea derivatives were investigated. The disubstituted phenyl derivatives, **9a**–**f**,

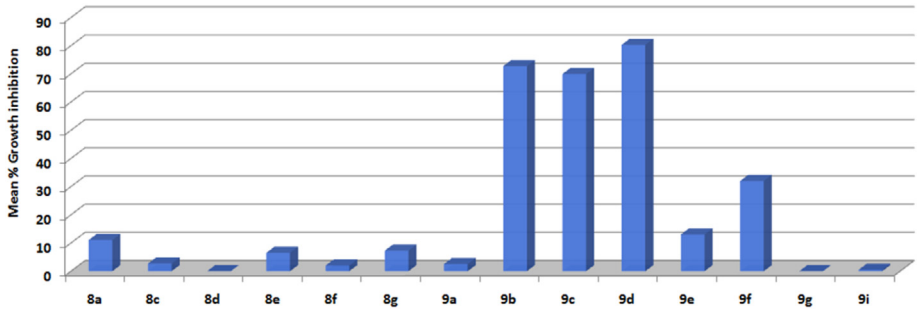

Fig. 2. Mean % growth inhibitions of the tested compounds over the full NCI 60 cell line panel.

showed higher mean % GI than the monosubstituted analogs **9g** and **9i**. Therefore, it could be concluded that the presence of dichloro, difluoro or chloro and trifluoromethyl substituents on the terminal phenyl ring of urea derivatives augment the anticancer activity, and this may be attributed to the resultant increase in compound lipophilicity, permeability and penetration into cancer cells and hence the cellular potency. In addition, compound **9b** with 2,4-difluorophenyl ring was significantly more potent (mean % GI = 72.74) than the corresponding dichloro homolog **9a** (mean % GI = 2.55), which denotes that the best substituent at 2,4-positions of the terminal phenyl is fluorine rather than chlorine. Regarding the 3,4-positions, it was observed that the best antiproliferative activity was achieved in case of combining the *m*-trifluoromethyl moiety with *p*-chlorophenyl (**9d**, mean % GI = 80.32) rather than the 3,4-dichlorophenyl derivative (**9f**, mean % GI = 32.0). A possible reason for this is the differences in the steric and/or electronic effects of trifluoromethyl group compared with chlorine group, and such assumption was strongly supported upon comparing the 3,5-bis-trifluoromethylphenyl urea **9c** (mean % GI = 69.95) with the dichlorophenyl analogs **9a** and **9f** (mean % GI = 2.55 and 32.00, respectively). Interestingly, it was found that the antitumor activity of compound **9e** (mean % GI = 13.04) was greatly lower than its positional isomer **9d** (mean % GI = 80.32), which points out that the 4-chloro-3-trifluoromethylphenyl terminal is better substitution pattern than 2-chloro-5-trifluoromethylphenyl, and may geometrically allow appropriate fitting of the molecule at the receptor site, and therefore improved antitumor activity. Upon comparing the antiproliferative activity of the 2-chloro substituted derivatives **9a** and **9e** (mean % GI = 2.55 and 13.04, respectively) with that of the 3,4-dichlorophenyl derivative **9f** (mean % GI = 32.00), it was revealed that incorporation of chlorine at the *ortho* position of the terminal phenyl is unfavorable for the activity. Among all of the examined derivatives, compounds **9b**–**d** showed the highest mean GI, and their effects on the percentages growth of the individual cell lines of the NCI-60 panel at 10 μM concentration are shown in Fig. 3.

Close examination of the findings presented in Fig. 3, revealed the broad spectrum anticancer activities of compounds **9b**–**d** over all the nine tested cancer types. The three compounds displayed strong antiproliferative activities (>80% inhibition) over 22, 16, and 25 cell lines, respectively. Furthermore, compounds **9b**–**d** exerted remarkable cytotoxic effects (minus percentages growth) against several cell lines. Of particular significance, compound **9d** exerted lethal activity over SNB-75 (CNS cancer), OVCAR-4 (ovarian cancer), and the renal carcinoma cells 786-0 and TK-10 with percentages growth values of −47.99%, −72.84%, −59.47%, and −29.79%, respectively. In addition to the previously mentioned 4 cell lines sensitive to **9d**, both compounds **9b** and **9c** manifested remarkable lethal activities against other cell lines. The colon cancer HCT-116, CNS cancer SF-539 and melanoma MALME-3M cell lines were found to be sensitive to compound **9b** (percentages growth values of −33.05%, −18.90% and −21.15%, respectively), while HOP-92 (NSCL), U251 (CNS cancer), OVACR-3 (ovarian cancer), and the renal carcinoma cells A498 and ACHN were proved to be highly sensitive toward compound **9c**. Compound **9d** showed broader cytotoxic effects over 15 of the tested NCI cell lines. Not only the most tested renal cancer (786-0, A498, ACHN, SN12C, TK-10 and UO-31), but also three breast cancer cell lines including MDA-MB-231, HS 578T and T-47D were highly sensitive to compound **9d**.

2.2.2.2. Five-dose testing. Compounds **9b**–**d** and **9f** with promising results in single-dose test and satisfying the criteria set by the NCI for activity in that preliminary assay were further tested in a five-dose testing mode at 10-fold dilution (100–0.01 μM) on the full panel. For each of these compounds, three response parameters; the IC_{50} (the concentration producing 50% GI, a measure of compound potency), TGI (the concentration producing 100% GI, a measure of compound efficacy) and LC_{50} (the concentration causing 50% lethality, a measure of compound efficacy and cytotoxicity) were determined. The IC_{50} values of those four compounds are showed in Table 2. The results of sorafenib as a reference compound were obtained from NCI Data Warehouse index [33], and are inserted in Table 2.

As illustrated in Table 2, the four tested compounds **9b**–**d** and **9f** showed high potency with one-digit micromolar IC_{50} values over most of the cell lines. Moreover, the target compounds exhibited superior potency than sorafenib against 36, 6, 12, and 5 cell lines, respectively. It was evident that the three fluorinated derivatives **9b**–**d** were much potent than the chlorinated compound **9f** regarding most of the cell lines, which implies the significance of fluorine for antiproliferative activity of this new set of compounds. Such finding was in agreement with the postulation that incorporation of fluorine may enhance the binding affinity to the target protein and thus improving the potency [34].

While sorafenib is originally used for treatment of renal cell carcinoma (RCC) [13,17], it was interesting to find that compounds **9b**–**d** were highly potent than sorafenib over the majority of RCC panel, particularly 786-0, A498, RXF393, and TK-10 cell lines. Of special interest, compound **9b** with 2,4-difluorophenyl ring exerted the highest potencies. Its IC_{50} values against both 786-0 and A498 cell line were 926 nM and 418 nM, three and six times more potent than sorafenib, respectively. Both compounds **9c** and **9d**, possessing the same *m*-trifluoromethylphenyl motif of sorafenib, displayed significant antiproliferative activity over the most sensitive RCC, A498 with low micromolar IC_{50} values (1.99 and 1.36 μM, respectively).

On the other hand, sorafenib was clinically investigated for treatment of ovarian cancer, however results demonstrated poor clinical benefit either as single agent or in combination therapy [35,36]. Therefore, it was of great significance to observe that compounds **9b**–**d** significantly surpassed the activity of sorafenib towards OVCAR-4 ovarian cancer cell. Again, compound **9b** was the best (IC_{50} = 897 nM) against OVACR-4, in addition to its equipotent activity (IC_{50} = 1.65 μM) over three ovarian cancer cell lines; OVACR-8, NCI/ADR-RES, and SK-OV-3.

From another perspective, sorafenib was interrogated for treatment of NSCL and showed significant clinical improvement [37,38]. In this regard, it is noteworthy to mention that compound **9b** showed profound antineoplastic activity overcoming sorafenib over all tested NSCL cancer cell lines, with IC_{50} values of 0.753–1.49 μM.

Besides the previously mentioned targeted cellular potencies of compound **9b**, it showed remarkable broad spectrum potency over other multiple cell lines like SR leukemia cell, HCT-116 and HCT-15 colon cancer cells with IC_{50} values of 0.41, 0.711 and 0.302 μM, respectively. Moreover, it was equipotent (IC_{50} = 0.78 μM) against both SNB-75 and U251 CNS cancer cells.

By referring to the efficacy parameters (TGI and LC_{50} values) of the target compounds presented in Table 3, it was demonstrated that the most potent compound **9b** was also efficacious towards SNB-75 CNS cancer cell, OVCAR-4 ovarian cancer cell, RXF393 renal carcinoma cell, and the breast cell line HS 5783 with TGI values of 1.74, 2.03, 2.99, and 3.99 μM, respectively. While compounds **9c** and **9d** showed the highest efficacies over the most of renal cancer cell lines, compound **9d** exerted remarkable efficacies against 786-0, A498, and TK-10 cell lines, being able to induce total growth inhibition (TGI) and 50% lethality (LC_{50}) at concentrations below 100 μM.

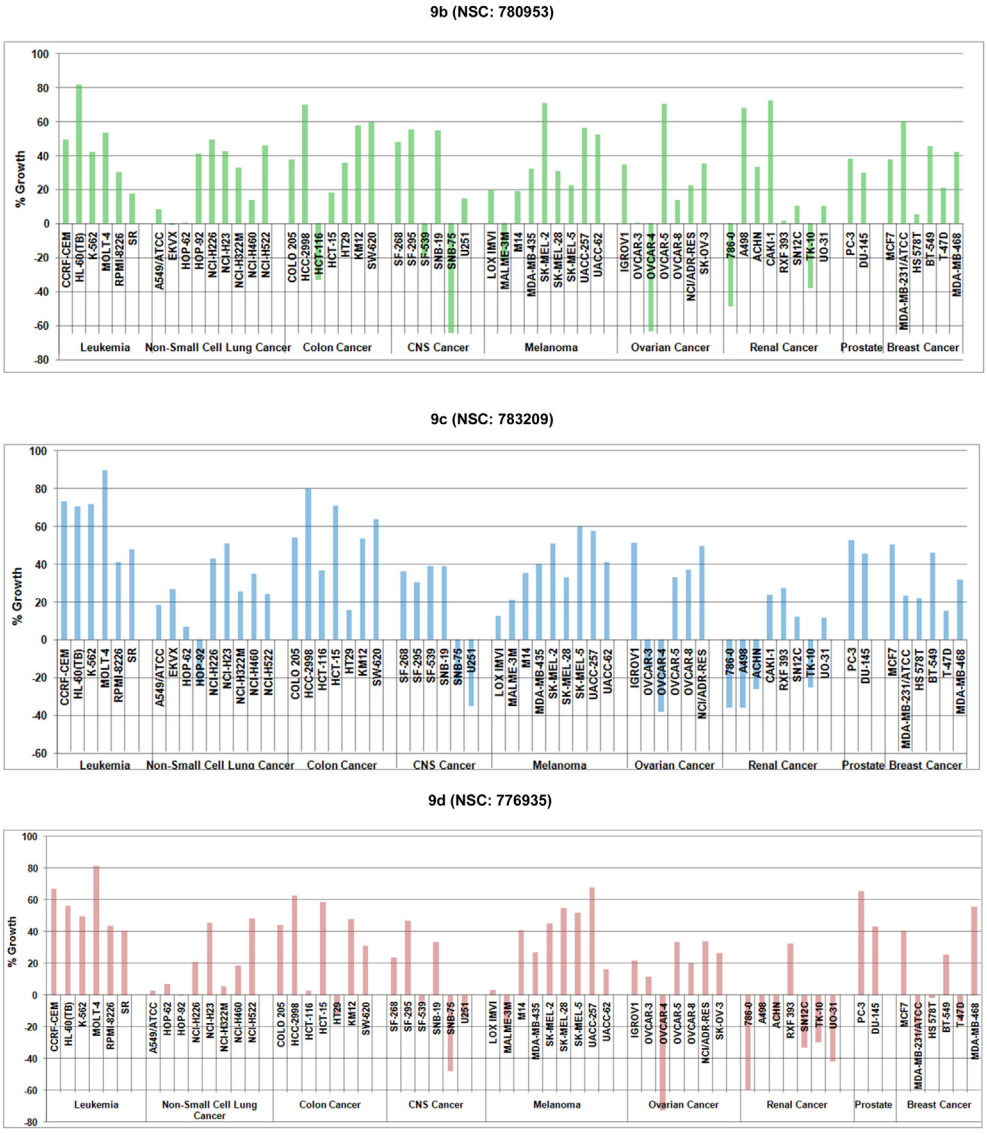

Fig. 3. % Growth of NCI 60 cell line panel upon treatment with compounds **9b**–**d** at 10 μM concentration.

2.3. *In vitro kinase screening*

In attempt to investigate the mechanism of action and the kinase inhibitory profile of this new set of compounds, compound **9d** which possesses most of the structural features of sorafenib (4-chloro-3-trifluoromethylphenyl, urea linker, and *N*-methylpicolinamide), and exhibited high potency and efficacy over renal cancer cell lines was tested at a single dose concentration of 10 μM over a panel of 41 oncogenic kinases at Reaction Biology Corporation (RBC, Malvern, PA, USA) [39]. As illustrated in Fig. 4, compound **9d** has shown highly potent inhibitory activity against C-RAF kinase with 96.3% inhibition, as well as inhibiting the mutant $BRAF^{V600E}$ (81.8% inhibition) at 10 μM. Meanwhile, it exerted moderate activity over MAPK14 kinase (51.8% inhibition) and modest activity towards the other kinases with inhibition percentage less than 40. Compound **9d** was further tested in a 10-dose testing mode to determine its IC_{50} values over $BRAF^{V600E}$ and C-RAF, and showed IC_{50} values of 316 nM and 61 nM, respectively. Interestingly, the compound **9d** was found to inhibit C-RAF 5 times more than $BRAF^{V600E}$.

Upon comparing compound **9d** with sorafenib in terms of the selectivity profile, compound **9d** displays a remarkable selectivity towards the RAF kinases, particularly $BRAF^{V600E}$ and C-RAF rather than the other protein kinases like VEGFR1, VEGFR2, FLT3, and c-Kit. Therefore, it was evident that our structural modifications, represented by compound **9d**, led to differential orientation and modulation of the binding affinities towards the different protein kinases and hence improving the selectivity profile.

Furthermore, we examined the inhibitory activity of compound **9b**, the 2,4-difluorophenyl congener of **9d**, against both $BRAF^{V600E}$ and C-RAF kinases. As revealed the results in Table 4, it exerted selective inhibitory effect for C-RAF rather $BRAF^{V600E}$ kinase. In comparison with compound **9d** (C-RAF IC_{50} = 61.0 nM), compound **9b** showed 13 fold reduced inhibitory activities (C-RAF IC_{50} = 807 nM), which indicates that the 4-chloro-3-trifluoromethylphenyl is favorable than 2,4-difluorophenyl and highlights its great significance for achieving RAF kinase inhibitory activity.

In consistence with the aforementioned biochemical assay results, compound **9d** exerted high potencies over the cell lines overexpressing mutant $BRAF^{V600E}$ like COLO 205 and HT29 colon cancer cell lines [40], and MALME-3M [40], SK-MEL-28 [41], SK-MEL-5 [41], and UACC-62 [42] melanoma cell lines. C-RAF is

Table 2
IC_{50} values (μM) of the tested compounds and sorafenib over NCI-60 cell line panel.[a,b]

Cell lines	IC_{50} value (μM)					Cell lines	IC_{50} value (μM)				
	9b	**9c**	**9d**	**9f**	**Sorafenib**		**9b**	**9c**	**9d**	**9f**	**Sorafenib**
Leukemia						**Melanoma**					
CCRF-CEM	>50	29.4	>100	NT	2.0	M14	**1.89**	10.2	5.00	NT	2.0
HL-60(TB)	NT	23.4	NT	NT	1.58	MDA-MB-435	**1.50**	4.70	3.12	NT	1.58
K-562	NT	9.29	>100	NT	3.16	SK-MEL-2	>50	12.7	7.18	3.18	1.58
MOLT-4	NT	35.9	>100	NT	3.16	SK-MEL-28	**1.42**	4.67	4.59	NT	2.0
RPMI-8226	2.20	NT	NT	NT	1.58	SK-MEL-5	**1.02**	6.20	2.62	NT	1.58
SR	**0.41**	13.0	3.22	NT	3.16	UACC-257	NT	1.32	>100	NT	2.0
Non-Small Cell Lung Cancer						UACC-62	NT	3.56	1.97	**1.47**	1.58
A549/ATCC	**1.01**	4.54	**2.83**	NT	3.16	**Ovarian Cancer**					
EKVX	NT	4.46	NT	NT	2.51	IGROV1	NT	NT	12.3	5.54	2.51
HOP-62	**0.903**	3.37	2.76	3.30	2.0	OVCAR-3	**1.26**	4.07	**2.84**	5.18	3.16
HOP-92	**1.49**	2.50	**1.51**	2.56	1.58	OVCAR-4	**0.897**	**2.37**	**1.17**	NT	3.16
NCI-H226	**0.94**	4.21	3.73	6.04	2.0	OVCAR-5	NT	13.3	3.85	NT	3.16
NCI-H23	NT	6.15	4.81	2.64	2.0	OVCAR-8	**1.65**	5.09	3.47	4.96	2.51
NCI-H322M	**1.16**	3.94	3.91	20.5	2.51	NCI/ADR-RES	**1.68**	5.62	3.88	3.07	2.51
NCI-H460	**0.753**	4.16	2.79	NT	2.51	SK-OV-3	**1.60**	2.99	3.78	2.73	2.51
NCI-H522	NA	6.65	14.7	2.03	2.0	**Renal Cancer**					
Colon Cancer						786-0	**0.926**	**2.41**	**1.89**	13.6	3.16
COLO 205	NT	10.8	4.36	NT	2.0	A498	**0.418**	**1.99**	**1.36**	5.94	2.51
HCC-2998	>50	15.5	>100	NT	3.16	ACHN	**2.13**	3.80	**1.66**	11.6	3.16
HCT-116	**0.711**	13.8	2.28	2.73	1.58	CAKI-1	**1.61**	10.1	4.28	4.12	3.16
HCT-15	**0.302**	18.1	NT	NT	2.51	RXF 393	**1.24**	**3.03**	**1.89**	5.09	3.16
HT29	**1.30**	3.51	2.04	NT	2.0	SN12C	**1.37**	5.27	2.62	3.41	2.51
KM12	NT	15.2	9.94	NT	1.58	TK-10	**1.03**	**3.22**	**2.17**	**2.70**	3.98
SW-620	NT	16.9	NT	NT	2.51	UO-31	NT	4.91	2.62	>100	2.51
CNS Cancer						**Prostate Cancer**					
SF-268	**1.90**	4.93	3.84	3.25	2.51	PC-3	NT	6.06	47.7	NT	2.0
SF-295	NT	3.69	2.16	3.00	1.58	DU-145	**1.28**	6.29	4.74	**2.39**	3.16
SF-539	**1.17**	6.68	2.60	89.1	1.58	**Breast Cancer**					
SNB-19	**1.30**	5.31	5.06	6.54	3.16	MCF7	**1.66**	7.43	5.91	NT	2.51
SNB-75	**0.788**	**2.38**	**1.09**	**2.50**	3.16	MDA-MB-231/ATCC	1.59	NT	1.67	1.59	1.26
U251	**0.783**	2.47	3.12	2.84	2.0	HS 578T	**1.40**	2.57	**1.73**	7.36	2.51
Melanoma						BT-549	>50	11.4	4.67	**2.59**	3.16
LOX IMVI	1.68	3.26	2.32	2.20	1.58	T-47D	**1.23**	4.13	**1.47**	3.28	1.58
MALME-3M	NT	2.62	2.61	2.23	2.0	MDA-MB-468	**1.83**	3.40	3.56	2.25	2.0

[a] Bold figures indicate superior potency than sorafenib, bold underlined figures refer to submicromolar IC_{50} values.
[b] NT, not tested.

Table 3
TGI and LC_{50} values (μM) of the tested compounds and sorafenib over the most sensitive cell lines.[a,b]

Cell lines	**9b**		**9c**		**9d**		**9f**		**Sorafenib**	
	TGI	LC_{50}	TGI	LC_{50}	TGI	LC_{50}	TGI	LC_{50}	TGI	LC_{50}
NSCL Caner										
HOP-92	NT	>50	6.27	29.5	5.75	61.80	9.42	67.00	5.01	31.6
CNS Cancer										
SNB-75	**1.74**	>50	14.9	>100	**2.63**	6.33	**7.28**	31.80	10.0	39.8
Ovarian Cancer										
OVCAR-4	**2.03**	NT	**7.51**	>100	**2.91**	NT	NT	>100	12.6	100
Renal Cancer										
786-0	NT	NT	**5.73**	24.6	**4.17**	9.20	35.70	94.00	10.0	50.1
A498	23.3	NT	**5.02**	25.3	**4.54**	51.70	30.90	>100	6.31	31.7
ACHN	>50	>50	16.4	69.0	**5.58**	>100	>100	>100	12.6	100
CAKI-1	>50	>50	57.3	>100	>100	>100	>100	>100	3.98	10.0
RXF 393	**2.99**	>50	9.48	33.5	**7.42**	45.40	24.30	93.00	10.0	39.8
SN12C	NT	>50	>100	>100	>100	>100	>100	>100	10.0	39.8
TK-10	NT	>50	11.5	44.8	**5.08**	17.00	**5.73**	19.40	10.0	50.1
Breast Cancer										
HS 5783	**3.99**	>50	13.5	>100	**7.58**	>100	74.40	>100	7.94	100
T-47D	NT	>50	31.1	>100	**5.14**	>100	>100	>100	7.94	31.7

[a] Bold figures refer to superior efficacies than sorafenib regarding TGI values, underlined figures indicate superior efficacies than sorafenib regarding LC_{50} values.
[b] NT, not tested.

commonly over-expressed in the absence of oncogenic mutations in 50% of RCC (50%) [43], and is associated with poor prognosis in ovarian cancer [44]. Therefore, the remarkable antiproliferative activities of **9b** and **9d** over a number of RCC and ovarian cancer cell lines may be attributed to C-RAF kinase inhibition. On the other hand, it is noticeable that the low inhibitory activity of compound **9b** over $BRAF^{V600E}$ could not justify its significant cellular potency over certain $BRAF^{V600E}$ dependent cell lines like HT29 colon cancer, SK-MEL-28 and SK-MEL-5 melanoma cell lines, which may indicate the existence of other underlying mechanisms responsible for the

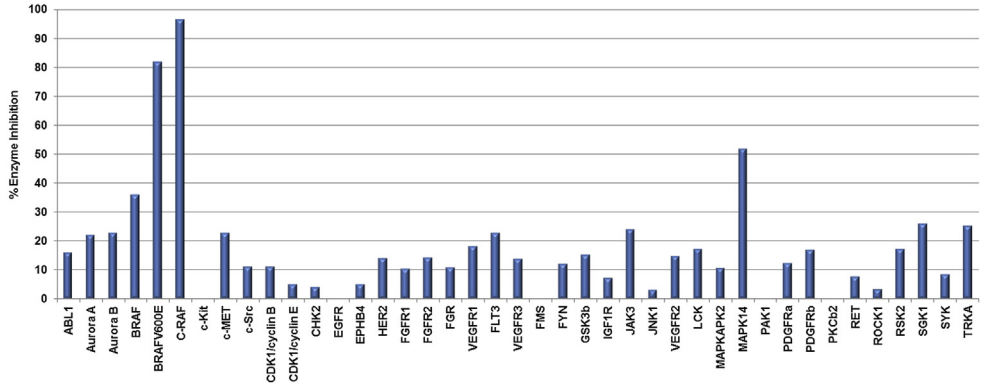

Fig. 4. Inhibition percentages of compound **9d** over a panel of 41 oncogenic kinases at 10 μM concentration.

Table 4
In vitro enzymatic activity of **9b**, **9d** and sorafenib over $BRAF^{V600E}$ and C-RAF kinases.

Compound no.	% Enzymatic inhibition[a] (IC_{50}, nM)[b]	
	$BRAF^{V600E}$	C-RAF
9b	9.72 (>10,000)	63.5 (807)
9d	81.8 (316)	96.3 (61.0)
Sorafenib	(38.0)	(6.00)

[a] Compounds were tested in single dose duplicate mode at a concentration of 10 μM.
[b] Compounds were tested in a 10-dose IC_{50} mode with 3-fold serial dilution starting at 100 μM.

antiproliferative activity of **9b** towards those cell lines.

From the previously mentioned cellular and biochemical assay results, it was clearly demonstrated that compound **9b** is a C-RAF kinase inhibitor with potent antiproliferative activity in terms of IC_{50} values against multiple cancer cell lines. While, compound **9d** is a dual selective $BRAF^{V600E}$ and C-RAF inhibitor with potent antiproliferative activity in terms of TGI values over several tumor cell lines. Such findings suggest the presence of additional mechanisms beside C-RAF kinase inhibition that control the anticancer activity of this new set of compounds.

2.4. Molecular docking study

In order to rationalize the observed RAF kinase inhibitory activity from a 3D structural perspective, **9d** was docked in the catalytic kinase domain of $BRAF^{V600E}$ (PDB accession code 1UWJ) [45], and C-RAF homology model. Fig. 5 illustrates the overlay of **9d** with the co-crystallized conformation of sorafenib. The docking model demonstrates a substantially similar binding mode for both compounds with the two homologous kinases. As an example, in case of $BRAF^{V600E}$, the mutual binding interactions include hydrogen bonds to (1) backbone amidic nitrogen and the aminocarbonyl oxygen of Cys532 in the hinge region *via* the picolinamide moiety, (2) the backbone amine of Asp594 through the carbonyl oxygen of urea, and (3) the side chain carboxylate of Glu501 through the urea NH. Besides, both **9d** and sorafenib showed hydrophobic interactions with the allosteric binding region, which were mediated by their trifluoromethylphenyl group. Interestingly, it was noticed that the quinoline ring of **9d**, corresponding to the phenyl group of sorafenib, was engaged in multiple hydrophobic and electrostatic interactions with various amino acid residues (like Lys483 and Thr529) in the gatekeeper region.

Similarly, compound **9d** showed perfect binding with both the active and allosteric sites of C-RAF kinase. The pyridylamide NH of **9d** was involved in hydrogen bonding interaction with the carbonyl oxygen of Cys424 in the hinge region, while the NH and oxygen of urea linker were tightly engaged in two hydrogen bonds with the carboxylate oxygen and amine group of Glu393 and Asp486 residues in the DFG loop, respectively. Moreover, several hydrophobic interactions (Pi–Pi T-shaped and Pi-alkyl) were observed between the quinoline core and gatekeeper residues (Val363, Lys375, and Phe487). Furthermore, the 4-chloro-3-trifluoromethylphenyl terminal of **9d** displayed hydrophobic interactions with Val396, Ile464, and Leu459 amino acid residues in the allosteric site. Taken together, it could be concluded that the structural features of **9d** allow profitable binding with $BRAF^{V600E}$ and C-RAF kinases.

Furthermore, to obtain some insights about the relatively superior enzymatic activity of **9d** rather **9b** towards $BRAF^{V600E}$, structural superimposition of both compounds in the catalytic kinase domain of $BRAF^{V600E}$ was carried out (detailed binding mode in Fig. 1 in the Supplementary data). As shown in Fig. 6, the *m*-trifluoromethylphenyl group of **9d** was deeply inserted into a hydrophobic subpocket in the allosteric binding region, associating with perfect orientation of the picolinamide end of the scaffold into the $BRAF^{V600E}$ kinase hinge region and formation of the crucial hydrogen bonds for binding. In contrast, the 2,4-difluorophenyl group of compound **9b** was little far from the allosteric binding site, resulting in relatively loose binding and improper positioning of the pyridyl amide motif into the hinge region. Such finding might provide a clue explaining the good activity of **9d** towards $B\text{-}RAF^{V600E}$ kinase in respect to **9b**.

2.5. Flow cytometry cell cycle analysis

To better understand the antiproliferative activity of the most potent urea derivatives, **9b** and **9d**, the cell cycle analysis was carried out on the highly sensitive renal carcinoma cell line (A498). It was incubated with **9b** and **9d** at 2.5 and 5.0 μM for 48 h, then the fractions (%) of cell cycle phases were determined by flow cytometry before a significant amount of cells underwent apoptosis (Fig. 7 and Table 5). The results indicated that both **9b** and **9d** induced dose dependent cell cycle arrest in both G2/M and S phases. As an example, compounds **9b** at 5.0 μM caused more accumulation of the cells in G2/M phase (26.6%) as well as S phase (36.0%) relative to control. Moreover, upon treatment of the A498 cell with the tested compounds at little higher concentrations than 5.0 μM, a massive increase of the cells population in sub G0/G1 phase (dead cells) was noticed, which is indicative of apoptosis.

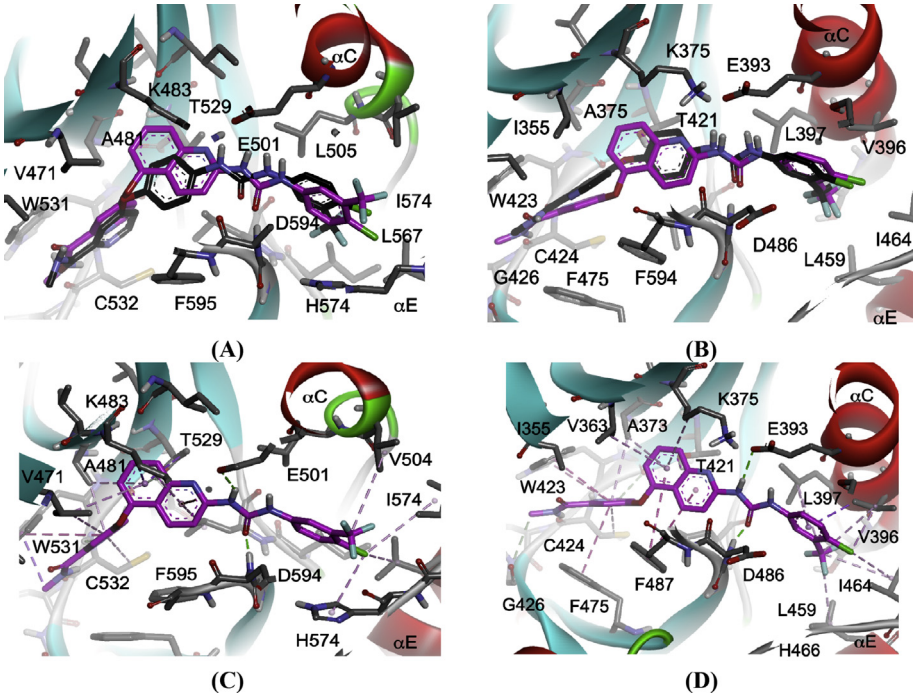

Fig. 5. Structural overlay of the docked pose of compound **9d** (magenta) and sorafenib (black) in the catalytic kinase domain of $BRAF^{V600E}$ (A) and C-RAF homology model (B). Detailed binding mode of compound **9d** in the catalytic kinase domain of $BRAF^{V600E}$ (C) and C-RAF homology model (D).

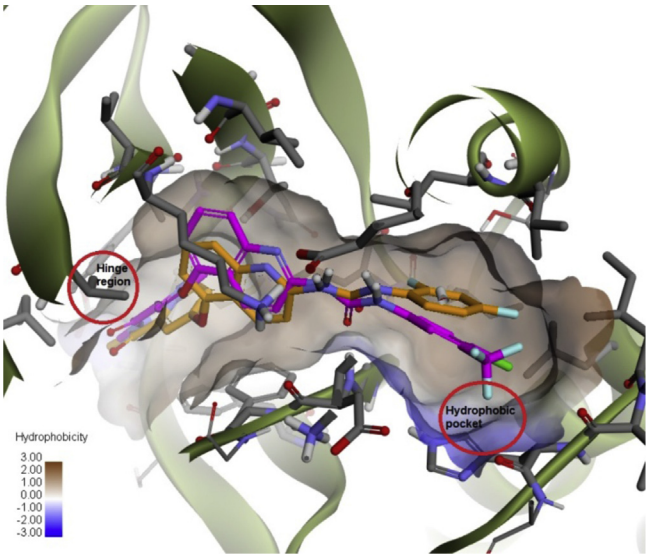

Fig. 6. Superimposition of the docked pose of compounds **9b** (orange) and **9d** (magenta) in the catalytic kinase domain of $BRAF^{V600E}$. (For interpretation of the references to color in this figure legend, the reader is referred to the web version of this article.)

2.6. Compliance to Lipinski's rule of five and in silico toxicity assessment

As a part of our study; the compliance of the most potent compounds **9b**–**d** and **9f**, to the Lipinski's rule of five was evaluated (Supplementary data). All compounds complied with these rules. With the aim to get some insights about the overall toxicity (mutagenic, tumorigenic, irritant, or reproductive effects) of the most active derivatives, Osiris program [46] was used as a predictive tool for toxicity. Interestingly, all compounds presented a low *in silico* toxicity risk profile (Supplementary data). Such finding strongly supported the anticancer experimental data described in this work revealing these compounds as promising candidates with low toxicity risk profile.

3. Conclusion

A new series of *N*-methyl picolinamide based 2-amido and ureido quinoline derivatives has been designed and synthesized as sorafenib analogs in this study. A selected group (14 compounds) was assessed for its antiproliferative activity over a panel of 60 cancer cell lines at 10 μM concentration at NCI. Among them, 2-quinolinyl urea compounds, **9b**–**d** and **9f** have exerted strong inhibitory activities and were further tested at 5-dose testing mode. A structure activity relationship (SAR) study has been established and revealed that for best activity the compounds should possess urea as a linker tethering the substituted terminal phenyl with C2 of quinoline scaffold. Moreover, the disubstituted phenyl group was more favorable for anticancer activity than the monosubstituted one. And, among the disubstituted phenyl moieties, 2,4-difluorophenyl (**9b**) and 4-chloro-3-trifluoromethylphenyl (**9d**) groups were the best substitution patterns. In the second place for good activity comes the 3,5-bis(trifluoromethylphenyl) group (**9c**). Compounds **9b** and **9d** were found to be the most potent derivatives with one-digit micromolar or submicromolar IC_{50} values over the majority of tested cell lines, including those sorafenib sensitive cells such as RCC, ovarian, and NSCL. Screening of compound **9d** over 41 cancer related kinases at a single dose concentration of 10 μM showed its highly selective inhibitory effects against both $BRAF^{V600E}$ and C-RAF kinases. Its analog, **9b**, was found to differentially inhibit C-RAF rather $BRAF^{V600E}$ kinase. Molecular docking of **9d** in $BRAF^{V600E}$ and C-RAF kinases revealed similar binding mode with that of sorafenib. Moreover, cell cycle analysis demonstrated the ability of **9b** and **9d** to induce cell cycle arrest at G2/M and S phase. The most active compounds showed good

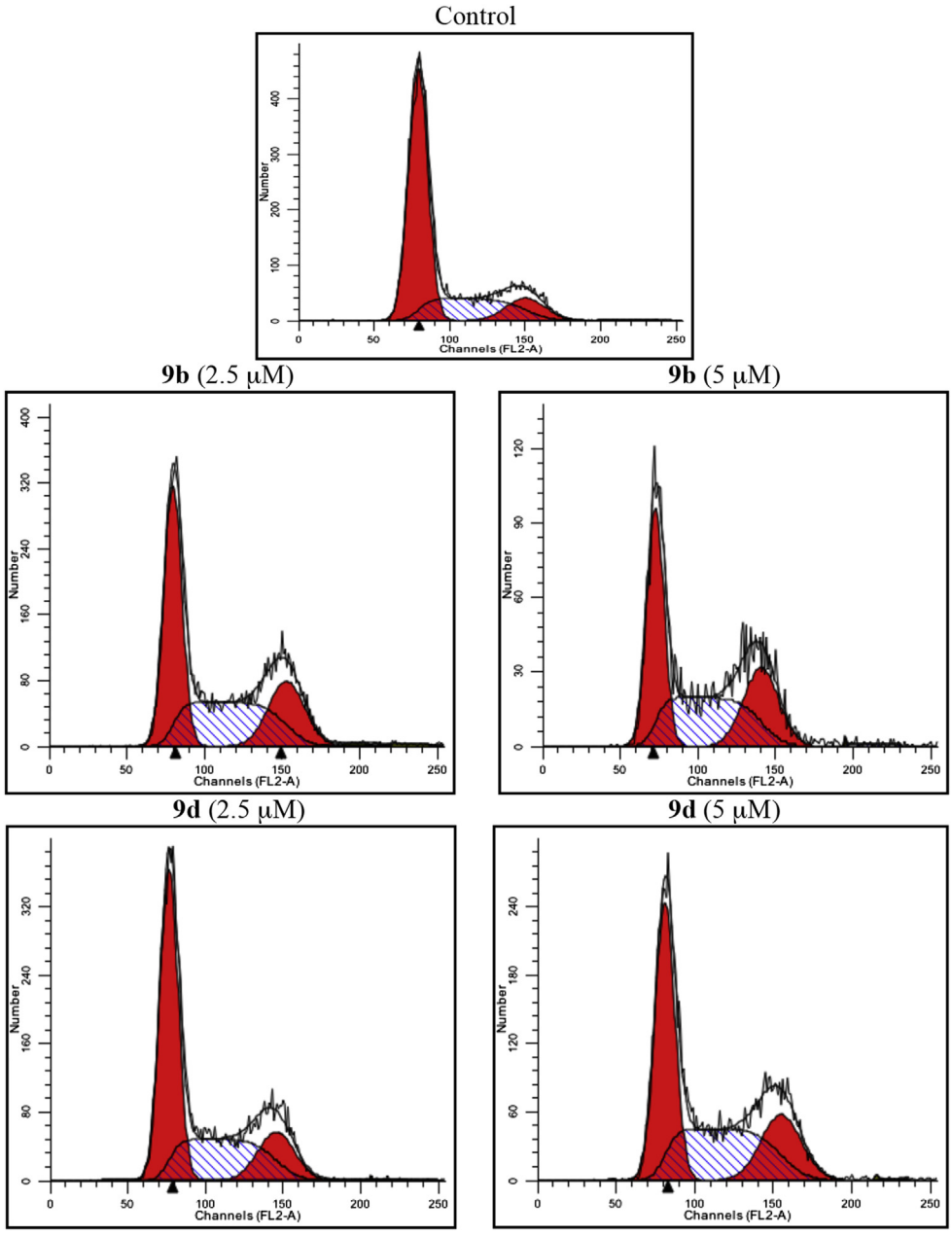

Fig. 7. Flow cytometric analysis of the A498 renal cancer cell line after treatment with compounds **9b** and **9d** at 2.5 and 5.0 μM for 48 h.

compliance to Lipinski's rule of five and low toxicity profile, affording new promising chemotherapeutic candidates that could be exploited for further development of potent anticancer agents.

Table 5
Cell cycle distribution of A498 cell line treated with **9b** and **9d**.

Compound no. (conc.)	% of cell cycle phases distribution		
	G1/G0	G2/M	S
Control	64.3	11.8	24.0
9b (2.5 μM)	42.2	21.3	36.5
9b (5 μM)	37.4	26.6	36.0
9d (2.5 μM)	52.5	16.4	31.1
9d (5 μM)	43.5	19.2	37.3

4. Experimental

4.1. General

Melting points were measured with a Thomas Hoover capillary melting point apparatus and were uncorrected. ^{1}H and ^{13}C NMR spectra were recorded on a Bruker Avance 300 or 400 MHz spectrometer, using appropriate deuterated solvents, as indicated. Chemical shifts (δ) are given in parts per million (ppm) upfield from tetramethylsilane (TMS) as internal standard, and s, d, t, and m are designated as singlet, doublet, triplet and multiplet, respectively. Coupling constants (J) are reported in hertz (Hz). Mass spectra were recorded on Waters Acquity UPLC/Synapt G2 QTOF MS mass

spectrometer. The reaction progress was monitored on TLC plate (Merck, silica gel 60 F_{254}), and flash column chromatography was carried out using silica gel (Merck, 230–400 mesh) and the indicated solvent system. Solvents and liquid reagents were transferred using hypodermic syringes. All solvents and reagents were commercially available and used without further purification.

4.2. 5-Methoxyquinoline (**1**)

A solution of 5-hydroxyquinoline (4.0 g, 27.6 mmol) in anhydrous DMF (60 mL) was cooled and then added slowly to NaH (1.33 g, 33.12 mmol, 60% dispersion in mineral oil) at 0 °C under argon atmosphere. The resulting mixture was stirred at the same temperature for 30 min. Methyl iodide (4.7 g, 33.12 mmol) was added dropwise to the suspension and the reaction mixture was allowed to warm to room temperature (rt) while stirring for additional 30 min. The reaction mixture was quenched with water (300 mL) and then extracted with diethyl ether (6 × 100 mL). The combined organic layers were washed with water and then brine, dried over anhydrous Na_2SO_4, filtered and the solvent was removed under reduced pressure to afford the title product as brown oil; yield: 4.03 g (92%); ^{1}H NMR (400 MHz, $CDCl_3$) δ 8.95 (dd, J = 4.2, 2.0 Hz, 1H), 8.62 (dd, J = 8.4, 1.2 Hz, 1H), 7.74 (d, J = 8.0 Hz, 1H), 7.65 (t, J = 8.4 Hz, 1H), 7.42 (dd, J = 8.4, 4.4 Hz, 1H), 6.90 (d, J = 8.0 Hz, 1H), 4.05 (s, 3H); ^{13}C NMR (100 MHz, $CDCl_3$) δ 155.17, 150.66, 148.70, 130.81, 129.37, 121.58, 120.85, 120.19, 104.22, 55.76.

4.3. 5-Methoxyquinoline-N-oxide (**2**) [30,31]

5-Methoxyquinoline (**1**) (4.03 g, 25.3 mmol) was dissolved in dichloromethane (DCM, 40 mL) under nitrogen and treated with *m*CPBA (70%; 6.56 g, 38.0 mmol) at 0 °C. The reaction mixture was stirred at rt for 6 h, then water (100 mL) was added and the aqueous phase was adjusted to alkaline pH upon addition of saturated aqueous sodium carbonate solution. The aqueous phase was extracted with DCM (3 × 150 mL) and the combined organic phases were washed with brine, dried over anhydrous Na_2SO_4, filtered, concentrated under reduced pressure and stored in refrigerator overnight to afford the desired product; yellow solid; yield: 4.085 g (92%); ^{1}H NMR (400 MHz, $CDCl_3$) δ 8.60 (dd, J = 6.0, 0.8 Hz, 1H), 8.34 (d, J = 9.2 Hz, 1H), 8.19 (d, J = 8.4 Hz, 1H), 7.70 (t, J = 7.6 Hz, 1H), 7.29 (t, J = 4.8 Hz, 1H), 6.99 (d, J = 7.6 Hz, 1H), 4.05 (s, 3H); ^{13}C NMR (100 MHz, $CDCl_3$) δ 155.60, 142.14, 136.48, 130.89, 123.31, 121.92, 119.74, 111.40, 106.59, 56.12; LC/MS (ESI$^+$) m/z = 175 (M^+).

4.4. 5-Methoxyquinolin-2(1H)-one (**3**)

p-Toluenesulfonyl chloride (5.55 g, 29.1 mol) was added portion wise at rt to a solution of compound **2** (4.09 g, 23.3 mmol) in 10% aqueous K_2CO_3 (60 mL) and DCM (60 mL) and the mixture was stirred at the same temperature for 18 h. Diethyl ether was added and the resultant precipitate was filtered, washed with diethyl ether and dried in oven at 65 °C for 2 h to furnish the title compound as light yellow solid; yield: 2.651 g (65%); ^{1}H NMR (400 MHz, $CDCl_3$) δ 12.15 (br. s, 1H), 8.25 (d, J = 9.6 Hz, 1H), 7.45 (t, J = 8.4 Hz, 1H), 7.04 (d, J = 8.4 Hz, 1H), 6.67 (t, J = 9.2 Hz, 2H), 3.97 (s, 3H); ^{13}C NMR (100 MHz, $CDCl_3$) δ 164.61, 156.09, 139.72, 135.74, 131.40, 119.67, 110.91, 108.66, 102.78, 55.73.

4.5. 2-Chloro-5-methoxyquinoline (**4**)

Phosphorus oxychloride (25.0 mL, 268.0 mmol) was added to compound **3** (2.65 g, 15.15 mmol) at rt and the resulting suspension was heated under reflux for 1 h. The reaction mixture was allowed to cool to rt, poured onto ice cold water (300 mL) and cautiously neutralized with diluted aqueous ammonium hydroxide in ice bath. The mixture was extracted with DCM (3 × 150 mL) and the combined organic layers were washed with brine, dried over anhydrous Na_2SO_4, filtered, and the solvent was removed under reduced pressure to afford the title compound; yellow solid; yield: 2.5 g (86%); ^{1}H NMR (400 MHz, $CDCl_3$) δ 8.46 (d, J = 8.8 Hz, 1H), 7.59 (dd, J = 10.0, 8.0 Hz, 2H), 7.31 (d, J = 8.4 Hz, 1H), 6.84 (t, J = 7.2 Hz, 1H), 3.97 (s, 3H); ^{13}C NMR (100 MHz, $CDCl_3$) δ 155.17, 151.03, 148.61, 133.97, 130.80, 121.07, 120.37, 119.20, 104.81, 55.77.

4.6. 5-Methoxyquinolin-2-amine (**5**)

A mixture of compound **4** (1.0 g, 5.2 mmol), acetamide (6.1 g, 103.3 mmol), and K_2CO_3 (3.6 g, 25.9 mmol) were fused at 200 °C for 15 h. The reaction mixture was cooled, diluted with water (15 mL) and extracted with ethyl acetate (3 × 35 mL). The combined organic layers were washed with brine, dried over anhydrous Na_2SO_4, filtered, and the solvent was removed under reduced pressure and the resultant residue was purified by flash column chromatography (hexane:ethyl acetate, 2:1 v/v) to afford the desired product as yellow solid; yield: 420 mg (47%); ^{1}H NMR (400 MHz, $CDCl_3$) δ 8.31 (d, J = 9.2 Hz, 1H), 7.48 (t, J = 8.4 Hz, 1H), 7.29 (d, J = 8.4 Hz, 1H), 6.68 (d, J = 8.8 Hz, 1H), 6.64 (d, J = 8.0 Hz, 1H), 5.29 (br. s, 2H), 3.96 (s, 3H); ^{13}C NMR (100 MHz, $CDCl_3$) δ 157.30, 155.55, 147.88, 133.10, 130.04, 117.85, 115.11, 110.52, 101.73, 55.59.

4.7. 5-Hydroxyquinolin-2-amine (**6**)

4.7.1. Method A

Compound **5** (1.0 g, 5.74 mmol) was dissolved in 48% aq. HBr (45 mL), and the resulting solution was heated under reflux for 8 h. The reaction mixture was then cooled, quenched with water (150 mL), and neutralized with saturated aqueous $NaHCO_3$ solution. The aqueous layer was extracted with ethyl acetate (5 × 100 mL) and the combined organic layers were washed with brine, dried over anhydrous Na_2SO_4, filtered, and the solvent was removed under reduced pressure producing the demethylated derivative as yellow solid; yield: 806 mg (88%).

4.7.2. Method B

To a cold solution of compound **5** (0.16 g, 0.92 mmol) in 5 mL of anhydrous DCM at 0 °C, 1 M solution of BBr_3 in DCM (7.1 mL, 6.8 mmol) was added drop wise under argon atmosphere. After complete addition, the reaction mixture was gradually warmed to rt and stirred for 18 h. The reaction was quenched with water (100 mL) and neutralized with saturated aqueous $NaHCO_3$ solution. The aqueous layer was extracted with ethyl acetate (3 × 50 mL) and the combined organic layers were washed with brine, dried over anhydrous Na_2SO_4, filtered, and the solvent was removed under reduced pressure to afford the title compound as yellow solid; yield: 73 mg (51%); ^{1}H NMR (300 MHz, Acetone-d_6) δ 8.40 (br. s + d, J = 9.0 Hz, 2H), 7.31 (t, J = 8.1 Hz, 1H), 7.18 (d, J = 8.3 Hz, 1H), 6.89 (d, J = 9.0 Hz, 1H), 6.73 (d, J = 7.5 Hz, 1H), 6.31 (br. s, 2H); ^{13}C NMR (75 MHz, Acetone-d_6) δ 158.36, 154.09, 148.55, 133.01, 130.05, 115.81, 114.51, 110.65, 105.67.

4.8. 4-((2-Aminoquinolin-5-yl)oxy)-N-methylpicolinamide (**7**)

To a stirred solution of compound **6** (1.0 g, 6.25 mmol) in anhydrous DMSO (25 mL), cesium carbonate (5.1 g, 15.63 mmol) and 4-chloro-*N*-methylpicolinamide (1.06 g, 6.25 mmol) were added and the reaction suspension was stirred for 15 min at rt. The reaction mixture was then heated at 135 °C for 5 h, cooled to rt, and quenched with water (150 mL). The resultant suspension was extracted with ethyl acetate (3 × 50 mL). The combined organic

layers were washed with water, brine solution, dried over anhydrous Na_2SO_4, filtered and the solvent was evaporated under reduced pressure yielding an oily residue that was purified by flash column chromatography using (0–100% ethyl acetate in hexane) to furnish the desired compound as yellow solid; yield: 1.36 g (73.9%); mp 189–191 °C; ^{1}H NMR (300 MHz, $CDCl_3$) δ 8.37 (d, J = 5.6 Hz, 1H), 8.00 (br. s, 1H, exchangeable with D_2O), 7.94 (d, J = 9.0 Hz, 1H), 7.77 (d, J = 2.3 Hz, 1H), 7.59–7.51 (m, 2H), 6.95–6.91 (m, 2H), 6.69 (d, J = 9.0 Hz, 1H), 4.94 (br. s, 2H, exchangeable with D_2O), 3.01 (d, J = 5.1 Hz, 3H); ^{13}C NMR (75 MHz, $CDCl_3$) δ 166.61, 164.49, 162.33, 157.43, 152.52, 149.84, 149.47, 131.91, 129.68, 124.03, 117.15, 113.75, 113.53, 112.15, 110.46, 26.13.

4.9. General procedure for synthesis of compounds **8a–g**

To a mixture of compound **7** (0.05 g, 0.17 mmol) and the appropriate aromatic carboxylic acid (0.34 mmol) in anhydrous DMF (2 mL) under argon atmosphere, *N*,*N*-diisoprpoylethylamine (DIPEA) (0.128 mL, 0.72 mmol) and HATU (0.168 g, 0.442 mmol) were added. The reaction mixture was stirred at rt for 24 h or at 80 °C for 5 h (for only **8g**), and then quenched with water (30 mL). The aqueous layer was extracted with ethyl acetate (3 × 20 mL) and the combined organic layers were washed with water and brine, dried over anhydrous Na_2SO_4, filtered, and the solvent was removed under reduced pressure. The resultant residue was purified by flash column chromatography, using the appropriate elution system to afford the target compounds **8a–g** in pure form.

4.9.1. 4-((2-(2,4-Dichlorobenzamido)quinolin-5-yl)oxy)-N-methylpicolinamide (**8a**)

Flash column chromatography was performed using 0–3% MeOH in DCM. White solid; yield 60.2%, mp 239–241 °C, ^{1}H NMR (400 MHz, DMSO-d_6) δ 11.58 (s, 1H), 8.81 (q, J = 4.8 Hz, 1H), 8.58 (dd, J = 5.6, 0.4 Hz, 1H), 8.38 (s, 2H), 7.84 (d, J = 5.6 Hz, 2H), 7.77 (d, J = 2.0 Hz, 1H), 7.68 (d, J = 8.4 Hz, 1H), 7.56 (dd, J = 8.4, 2.0 Hz, 1H), 7.43–7.39 (m, 2H), 7.26 (dd, J = 5.6, 2.4 Hz, 1H), 2.80 (d, J = 4.8 Hz, 3H); ^{13}C NMR (75 MHz, DMSO-d_6) δ 166.20, 166.00, 164.13, 153.13, 152.46, 151.14, 149.26, 148.22, 135.60, 135.53, 132.96, 131.99, 131.73, 130.94, 129.57, 127.80, 125.73, 119.88, 116.83, 115.82, 114.67, 109.55, 26.47.

4.9.2. 4-((2-(3,5-Dichlorobenzamido)quinolin-5-yl)oxy)-N-methylpicolinamide (**8b**)

Flash column chromatography was performed using 0–1% MeOH in DCM. White solid; yield 23.4%; mp 273–275 °C; ^{1}H NMR (300 MHz, DMSO-d_6) δ 11.53 (br. s, 1H), 8.81 (q, J = 4.8 Hz, 1H), 8.56 (d, J = 5.5 Hz, 1H), 8.38–8.30 (m, 2H), 8.08 (d, J = 1.8 Hz, 2H), 7.90–7.81 (m, 3H), 7.41 (dd, J = 8.3, 2.5 Hz, 2H), 7.25 (dd, J = 5.6, 2.6 Hz, 1H), 2.78 (d, J = 4.8 Hz, 3H); ^{13}C NMR (75 MHz, DMSO-d_6) δ 166.18, 164.51, 164.12, 153.14, 152.79, 152.68, 151.14, 149.28, 148.23, 137.54, 134.71, 132.69, 131.91, 130.88, 127.55, 126.30, 125.71, 119.89, 116.90, 116.48, 114.67, 109.56, 26.47.

4.9.3. 4-((2-(3,5-Bis(trifluoromethyl)benzamido)quinolin-5-yl)oxy)-N-methylpicolinamide (**8c**)

Flash column chromatography was performed using 0–1% MeOH in DCM. White solid; yield 57%; mp 259–260 °C; ^{1}H NMR (400 MHz, DMSO-d_6) δ 11.87 (br. s, 1H), 8.81 (q, J = 4.8 Hz, 1H), 8.72 (s, 2H), 8.58 (d, J = 5.6 Hz, 1H), 8.41 (s, 3H), 7.92–7.84 (m, 2H), 7.45 (d, J = 2.4 Hz, 1H), 7.43 (dd, J = 7.2, 1.6 Hz, 1H), 7.27 (dd, J = 5.6, 2.4 Hz, 1H), 2.80 (d, J = 5.2 Hz, 3H); ^{13}C NMR (100 MHz, DMSO-d_6) δ 166.17, 164.12, 153.11, 152.95, 152.75, 151.11, 149.27, 146.89, 141.21, 133.22, 131.45, 131.12, 131.07, 125.30, 125.09, 122.38, 119.79, 118.50, 116.40, 116.14, 114.81, 114.66, 109.51, 26.46.

4.9.4. 4-((2-(4-Chloro-3-(trifluoromethyl)benzamido)quinolin-5-yl)oxy)-N-methylpicolinamide (**8d**)

Flash column chromatography was performed using (hexane:ethyl acetate, 2:1 to 1:1 v/v). White solid; yield 85%; mp 223–225 °C; ^{1}H NMR (400 MHz, $CDCl_3$) δ 8.94 (br. s, 1H), 8.54 (s, 1H), 8.47 (d, J = 5.6 Hz, 1H), 8.37 (d, J = 9.2 Hz, 2H), 8.13 (d, J = 8.0 Hz, 1H), 8.05 (d, J = 4.8 Hz, 1H), 7.78 (d, J = 2.8 Hz, 2H), 7.73–7.69 (m, 2H), 7.20 (d, J = 7.6 Hz, 1H), 7.08 (dd, J = 5.6, 2.4 Hz, 1H), 3.04 (d, J = 5.2 Hz, 3H); ^{13}C NMR (100 MHz, $CDCl_3$) δ 166.22, 164.35, 152.65, 150.02, 149.46, 136.86, 134.14, 133.16, 132.83, 132.17, 131.48, 130.20, 129.45, 129.13, 126.96, 126.42, 125.24, 124.36, 123.71, 115.96, 114.71, 114.31, 110.23, 26.15.; HRMS (ESI-TOF) m/z calcd for $C_{24}H_{16}ClF_3N_4O_3Na$ $[M+Na]^+$: 523.0761, found: 523.0759.

4.9.5. 6-Chloro-N-(5-((2-(methylcarbamoyl)pyridin-4-yl)oxy)quinolin-2-yl)picolinamide (**8e**)

Flash column chromatography was performed using 0–1% MeOH in DCM. White solid; yield 91.7%; mp 242–243 °C; ^{1}H NMR (400 MHz, DMSO-d_6) δ 10.53 (s, 1H), 8.80 (q, J = 4.8 Hz, 1H), 8.58 (d, J = 5.6 Hz, 1H), 8.48 (q, J = 9.2 Hz, 2H), 8.25–8.18 (m, 2H), 7.94–7.85 (m, 3H), 7.46 (d, J = 2.8 Hz, 1H), 7.43 (dd, J = 7.2, 1.2 Hz, 1H), 7.27 (dd, J = 5.6, 2.4 Hz, 1H), 2.80 (d, J = 4.8 Hz, 3H); ^{13}C NMR (100 MHz, DMSO-d_6) δ 166.17, 164.16, 161.84, 153.14, 151.29, 151.17, 149.80, 149.74, 149.32, 148.27, 142.52, 133.44, 131.14, 128.93, 125.80, 122.34, 120.09, 116.91, 115.04, 114.66, 109.74, 26.31.

4.9.6. N-(5-((2-(Methylcarbamoyl)pyridin-4-yl)oxy)quinolin-2-yl)quinoline-6-carboxamide (**8f**)

Flash column chromatography was performed using 0–1% MeOH in DCM. White solid; yield 66%; mp 187–190 °C, ^{1}H NMR (400 MHz, DMSO-d_6) δ 11.54 (s, 1H), 9.05 (dd, J = 4.0, 1.6 Hz, 1H), 8.85 (d, J = 2.0 Hz, 1H), 8.82 (q, J = 5.2 Hz, 1H), 8.59 (d, J = 5.6 Hz, 1H), 8.55 (dd, J = 8.4, 1.2 Hz, 1H), 8.47–8.38 (m, 2H), 8.35 (dd, J = 8.8, 2.0 Hz, 1H), 8.15 (d, J = 8.8 Hz, 1H), 7.93–7.84 (m, 2H), 7.68 (dd, J = 8.0, 4.0 Hz, 1H), 7.46 (d, J = 2.4 Hz, 1H), 7.42 (dd, J = 7.2, 1.2 Hz, 1H), 7.28 (dd, J = 5.6, 2.8 Hz, 1H), 2.80 (d, J = 4.8 Hz, 3H); ^{13}C NMR (100 MHz, DMSO-d_6) δ 166.69, 166.21, 164.15, 153.15, 152.99, 151.14, 149.50, 149.31, 148.34, 137.85, 132.60, 131.99, 130.80, 130.04, 129.52, 128.72, 127.46, 125.65, 122.76, 119.81, 116.49, 114.67, 109.58, 26.48.

4.9.7. 4-((2-(2,3-Dihydrobenzo[b][1,4]dioxine-6-carboxamido)quinolin-5-yl)oxy)-N-methylpicolinamide (**8g**)

Flash column chromatography was performed using (hexane:ethyl acetate, 2:1 to 1:1 v/v). White solid; yield 35.7%; mp 107–110 °C; ^{1}H NMR (300 MHz, $CDCl_3$) δ 8.81 (br. s, 1H), 8.55 (d, J = 9.2 Hz, 1H), 8.42 (d, J = 5.6 Hz, 1H), 8.28 (d, J = 9.3 Hz, 1H), 8.01 (d, J = 4.4 Hz, 1H), 7.75–7.75 (m, 2H), 7.66 (t, J = 7.6 Hz, 1H), 7.55 (d, J = 2.1 Hz, 1H), 7.49 (dd, J = 8.4, 2.2 Hz, 1H), 7.13 (dd, J = 7.5, 0.8 Hz, 1H), 7.01 (dd, J = 5.6, 2.6 Hz, 1H), 6.97 (d, J = 8.4 Hz, 1H), 4.33 (d, J = 2.6 Hz, 4H), 3.01 (d, J = 5.1 Hz, 3H); ^{13}C NMR (75 MHz, $CDCl_3$) δ 166.34, 165.23, 164.40, 152.61, 152.05, 149.98, 149.41, 148.14, 147.50, 143.72, 132.75, 129.90, 127.10, 125.19, 120.90, 120.15, 117.59, 117.12, 115.61, 114.91, 114.15, 110.35, 64.65, 64.21, 26.16.

4.10. General procedure for synthesis of compounds **9a–k**

A solution of the suitable aryl isocyanate (0.187 mmol) in anhydrous DCM (2 mL) was added drop wise to a stirred solution of compound **7** (0.05 g, 0.170 mmol) in DCM (4 mL) under argon atmosphere at 0 °C. The reaction mixture was stirred at rt for 24 h, then the resulting solid was collected by filtration, washed with DCM and dried to yield the target compounds **9a–k** in pure form.

*4.10.1. 4-((2-(3-(2,4-Dichlorophenyl)ureido)quinolin-5-yl)oxy)-N-methylpicolinamide (**9a**)*

White solid; yield 100%; mp 246–248 °C; ^{1}H NMR (300 MHz, DMSO-d_6) δ 12.41 (br. s, 1H), 10.57 (s, 1H), 8.80 (q, J = 4.8 Hz, 1H), 8.55 (d, J = 5.6 Hz, 1H), 8.45 (d, J = 9.0 Hz, 1H), 8.26 (d, J = 9.1 Hz, 1H), 7.85–7.83 (m, 2H), 7.75 (d, J = 2.4 Hz, 1H), 7.46 (dd, J = 8.9, 2.3 Hz, 1H), 7.42 (d, J = 2.5 Hz, 1H), 7.34–7.29 (m, 2H), 7.22 (q, J = 2.6 Hz, 1H), 2.78 (d, J = 4.8 Hz, 3H); ^{13}C NMR (75 MHz, DMSO-d_6) δ 165.65, 163.62, 152.60, 151.92, 150.62, 148.97, 146.12, 135.01, 132.89, 131.00, 128.66, 127.80, 126.83, 123.89, 122.92, 122.31, 117.85, 115.88, 114.37, 114.15, 109.13, 25.97; HRMS (ESI-TOF) m/z calcd for $C_{23}H_{17}Cl_2N_5O_3Na$ $[M+Na]^+$: 504.0606, found: 504.0596.

*4.10.2. 4-((2-(3-(2,4-Difluorophenyl)ureido)quinolin-5-yl)oxy)-N-methylpicolin-amide (**9b**)*

White solid; yield 96%; mp 253–255 °C; ^{1}H NMR (400 MHz, DMSO-d_6) δ 12.48 (br. s, 1H), 10.46 (s, 1H), 8.79 (q, J = 4.8 Hz, 1H), 8.56 (d, J = 5.6 Hz, 1H) 8.37–8.30 (m, 1H), 8.26 (d, J = 9.2 Hz, 1H), 7.84 (t, J = 8.0 Hz, 1H), 7.76 (d, J = 8.4 Hz, 1H), 7.44 (td, J = 8.6, 2.8 Hz, 2H), 7.34 (t, J = 8.4 Hz, 2H), 7.23 (dd, J = 5.6, 2.4 Hz, 1H), 7.12 (t, J = 8.8 Hz, 1H), 2.80 (d, J = 4.8 Hz, 3H); ^{13}C NMR (100 MHz, DMSO-d_6) δ 166.14, 164.15, 153.33, 153.13, 152.54, 151.16, 149.49, 146.56, 133.23, 131.39, 124.36, 124.16, 122.10, 118.28, 116.30, 114.79, 111.93, 111.63, 109.66, 104.72, 104.31, 104.11, 26.49; HRMS (ESI-TOF) m/z calcd for $C_{23}H_{17}F_2N_5O_3Na$ $[M+Na]^+$: 472.1197, found: 472.1200.

*4.10.3. 4-((2-(3-(3,5-Bis(trifluoromethyl)phenyl)ureido)quinolin-5-yl)oxy)-N-methylpicolinamide (**9c**)*

White solid; yield 89%; mp 258–260 °C; ^{1}H NMR (400 MHz, DMSO-d_6) δ 11.98 (br. s, 1H), 10.43 (br. s, 1H), 8.80 (q, J = 4.4 Hz, 1H), 8.57 (d, J = 5.6 Hz, 1H), 8.36 (s, 2H), 8.28 (d, J = 9.2 Hz, 1H), 8.03 (d, J = 8.4 Hz, 1H), 7.85 (t, J = 8.0 Hz, 1H), 7.77 (s, 1H), 7.53 (d, J = 9.2 Hz, 1H), 7.41 (d, J = 2.4 Hz, 1H), 7.35 (dd, J = 7.8, 0.8 Hz, 1H), 7.25 (q, J = 2.4 Hz, 1H), 2.79 (d, J = 5.2 Hz, 3H); ^{13}C NMR (100 MHz, DMSO-d_6) δ 166.19, 164.12, 153.11, 152.97, 152.77, 151.12, 149.27, 146.92, 141.22, 133.26, 131.45, 131.13, 125.35, 125.10, 122.39, 119.86, 118.52, 116.45, 114.84, 114.68, 109.50, 26.47; HRMS (ESI-TOF) m/z calcd for $C_{25}H_{17}F_6N_5O_3Na$ $[M+Na]^+$: 572.1134, found: 572.1145.

*4.10.4. 4-((2-(3-(4-Chloro-3-(trifluoromethyl)phenyl)ureido) quinolin-5-yl)oxy)-N-methylpicolinamide (**9d**)*

White solid; yield 88%; mp 240–242 °C; ^{1}H NMR (400 MHz, DMSO-d_6) δ 11.97 (br. s, 1H), 10.39 (br. s, 1H), 8.81 (q, J = 4.8 Hz, 1H), 8.57 (d, J = 5.6 Hz, 1H), 8.35 (d, J = 2.4 Hz, 1H), 8.28 (d, J = 9.6 Hz, 1H), 8.00 (d, J = 8.8 Hz, 1H), 7.90–7.82 (m, 2H), 7.71 (d, J = 8.8 Hz, 1H), 7.52 (d, J = 9.2 Hz, 1H), 7.42 (d, J = 2.4 Hz, 1H), 7.35 (d, J = 7.2 Hz, 1H), 7.25 (dd, J = 5.6, 2.8 Hz, 1H), 2.79 (d, J = 4.8 Hz, 3H); ^{13}C NMR (75 MHz, DMSO-d_6) δ 166.16, 164.12, 153.12, 153.07, 152.59, 151.10, 149.33, 146.84, 138.74, 133.18, 132.56, 131.07, 125.07, 124.79, 124.05, 118.43, 118.17, 116.31, 114.82, 114.66, 109.55, 26.46; HRMS (ESI-TOF) m/z calcd for $C_{24}H_{17}ClF_3N_5O_3Na$ $[M+Na]^+$: 538.0870, found: 538.0862.

*4.10.5. 4-((2-(3-(2-Chloro-5-(trifluoromethyl)phenyl)ureido) quinolin-5-yl)oxy)-N-methylpicolinamide (**9e**)*

White solid; yield 90.2%; mp 283–285 °C; ^{1}H NMR (400 MHz, DMSO-d_6) δ 12.51 (br. s, 1H), 10.57 (s, 1H), 8.84 (d, J = 2.0 Hz, 1H), 8.69 (q, J = 4.4 Hz, 1H), 8.56 (d, J = 5.6 Hz, 1H), 8.28 (d, J = 9.2 Hz, 1H), 7.89–7.82 (m, 3H), 7.49 (d, J = 1.6 Hz, 1H), 7.47 (d, J = 2.4 Hz, 1H), 7.38 (d, J = 8.8 Hz, 1H), 7.33 (dd, J = 7.2, 1.2 Hz, 1H), 7.23 (dd, J = 5.6, 2.4 Hz, 1H), 2.81 (d, J = 4.8 Hz, 3H); ^{13}C NMR (100 MHz, DMSO-d_6) δ 166.12, 164.16, 153.24, 153.06, 152.58, 151.09, 149.59, 146.66, 137.29, 133.40, 131.43, 130.92, 129.03, 128.72, 126.49, 124.35, 120.62, 118.45, 117.91, 116.28, 114.90, 114.65, 109.75, 26.42; HRMS (ESI-TOF) m/z calcd for $C_{24}H_{17}ClF_3N_5O_3Na$ $[M+Na]^+$: 538.0870, found: 538.0867.

*4.10.6. 4-((2-(3-(3,4-Dichlorophenyl)ureido)quinolin-5-yl)oxy)-N-methylpicolinamide (**9f**)*

White solid; yield 91.6%; mp 234–236 °C; ^{1}H NMR (400 MHz, DMSO-d_6) δ 11.92 (s, 1H), 10.34 (s, 1H), 8.80 (q, J = 4.6 Hz, 1H), 8.57 (dd, J = 5.8, 0.3 Hz, 1H), 8.27 (dd, J = 9.1, 0.5 Hz, 1H), 8.13–8.12 (m, 1H), 8.01 (d, J = 8.5 Hz, 1H), 7.83 (t, J = 7.8 Hz, 1H), 7.62 (s, 2H), 7.47 (d, J = 9.1 Hz, 1H), 7.42 (d, J = 2.5 Hz, 1H), 7.34 (dd, J = 7.7, 0.8 Hz, 1H), 7.24 (dd, J = 5.6, 2.6 Hz, 1H), 2.79 (d, J = 4.8 Hz, 3H); ^{13}C NMR (75 MHz, DMSO-d_6) δ 166.18, 164.12, 153.12, 152.51, 151.12, 149.32, 146.82, 139.35, 133.23, 131.70, 131.18, 131.12, 125.15, 124.84, 120.82, 119.98, 118.40, 116.37, 114.83, 114.67, 109.54, 26.47; HRMS (ESI-TOF) m/z calcd for $C_{23}H_{16}Cl_2N_5O_3$ $[M-H]^+$: 480.0636, found: 480.0627.

*4.10.7. 4-((2-(3-(4-Chlorophenyl)ureido)quinolin-5-yl)oxy)-N-methylpicolinamide (**9g**)*

White solid; yield 85%; mp 248–250 °C; ^{1}H NMR (400 MHz, DMSO-d_6) δ 11.83 (s, 1H), 10.23 (s, 1H), 8.80 (q, J = 4.4 Hz, 1H), 8.55 (d, J = 5.6 Hz, 1H), 8.24 (d, J = 8.8 Hz, 1H), 7.94 (d, J = 8.4 Hz, 1H), 7.81 (t, J = 8.0 Hz, 1H), 7.73 (d, J = 8.8 Hz, 2H), 7.46–7.40 (m, 4H), 7.32 (d, J = 7.2 Hz, 1H), 7.23 (dd, J = 5.6, 2.8 Hz, 1H), 2.79 (d, J = 4.8 Hz, 3H); ^{13}C NMR (100 MHz, DMSO-d_6) δ 166.17, 164.13, 153.28, 153.11, 152.47, 151.10, 149.35, 146.85, 138.18, 133.08, 131.07, 129.27, 129.07, 126.95, 124.95, 121.18, 120.29, 118.31, 116.21, 114.83, 114.65, 109.58, 26.47; HRMS (ESI-TOF) m/z calcd for $C_{23}H_{18}ClN_5O_3Na$ $[M+Na]^+$: 470.0996, found: 470.0985.

*4.10.8. 4-((2-(3-(4-Bromophenyl)ureido)quinolin-5-yl)oxy)-N-methylpicolinamide (**9h**)*

White solid; yield 93.3%; mp 261–264 °C; ^{1}H NMR (400 MHz, DMSO-d_6) δ 11.82 (s, 1H), 10.24 (s, 1H), 8.80 (q, J = 4.4 Hz, 1H), 8.57 (d, J = 5.6 Hz, 1H), 8.25 (d, J = 9.2 Hz, 1H), 7.96 (d, J = 8.4 Hz, 1H), 7.82 (t, J = 8.0 Hz, 1H), 7.71–7.67 (m, 2H), 7.56–7.54 (m, 2H), 7.47 (d, J = 9.2 Hz, 1H), 7.43 (d, J = 2.8 Hz, 2H), 7.33 (d, J = 7.4 Hz, 1H), 7.24 (dd, J = 5.6, 2.4 Hz, 1H), 2.79 (d, J = 4.8 Hz, 3H); ^{13}C NMR (100 MHz, DMSO-d_6) δ 166.18, 164.12, 153.28, 153.13, 152.46, 151.12, 149.37, 146.87, 138.62, 132.18, 131.10, 124.97, 121.59, 118.34, 116.25, 114.89, 114.85, 114.66, 109.58, 26.47; HRMS (ESI-TOF) m/z calcd for $C_{23}H_{18}BrN_5O_3Na$ $[M+Na]^+$: 514.0491, found: 514.0490.

*4.10.9. 4-((2-(3-(4-Fluorophenyl)ureido)quinolin-5-yl)oxy)-N-methylpicolinamide (**9i**)*

White solid; yield 86%; mp 241–243 °C; ^{1}H NMR (400 MHz, DMSO-d_6) δ 11.75 (s, 1H), 10.20 (s, 1H), 8.81 (q, J = 4.8 Hz, 1H), 8.57 (d, J = 5.6 Hz, 1H), 8.25 (dd, J = 9.2, 0.8 Hz, 1H), 7.96 (d, J = 8.4 Hz, 1H), 7.82 (t, J = 8.0 Hz, 1H), 7.74–7.71 (m, 2H), 7.45 (d, J = 9.2 Hz, 1H), 7.42 (d, J = 2.4 Hz, 1H), 7.33 (dd, J = 7.6, 0.8 Hz, 1H), 7.25-7.23 (m, 3H), 2.79 (d, J = 5.2 Hz, 3H); ^{13}C NMR (100 MHz, DMSO-d_6) δ 166.20, 164.13, 158.42, 153.39, 153.12, 152.58, 151.12, 149.36, 146.90, 135.54, 133.07, 131.09, 124.99, 121.46, 118.28, 116.23, 116.09, 115.86, 114.77, 109.56, 26.47; HRMS (ESI-TOF) m/z calcd for $C_{23}H_{18}FN_5O_3Na$ $[M+Na]^+$: 454.1292, found: 454.1277.

*4.10.10. N-Methyl-4-((2-(3-(4-(trifluoromethyl)phenyl)ureido) quinolin-5-yl)oxy)picolinamide (**9j**)*

White solid; yield 95.7%; mp 271–273 °C; ^{1}H NMR (400 MHz, DMSO-d_6) δ 11.99 (s, 1H), 10.31 (s, 1H), 8.80 (q, J = 4.9 Hz, 1H), 8.57 (d, J = 5.6 Hz, 1H), 8.27 (d, J = 9.3 Hz, 1H), 7.97 (d, J = 8.4 Hz, 1H), 7.91 (d, J = 8.5 Hz, 2H), 7.83 (t, J = 7.8 Hz, 1H), 7.72 (d, J = 8.6 Hz, 2H), 7.50 (d, J = 9.1 Hz, 1H), 7.43 (d, J = 2.5 Hz, 1H), 7.34 (dd, J = 7.6, 0.7 Hz, 1H), 7.24 (dd, J = 5.6, 2.6 Hz, 1H), 2.80 (d, J = 4.8 Hz, 3H); ^{13}C NMR (100 MHz, DMSO-d_6) δ 166.17, 164.15, 153.19, 153.12, 152.48, 151.12, 149.38, 142.90, 133.22, 131.15, 126.70, 126.65, 124.98, 123.61, 123.57, 123.26, 119.52, 118.43, 116.33, 114.84, 114.67, 109.58, 26.46;

HRMS (ESI-TOF) *m/z* calcd for $C_{24}H_{18}F_3N_5O_3Na$ $[M+Na]^+$: 504.1260, found: 504.1258.

4.10.11. N-Methyl-4-((2-(3-(naphthalen-1-yl)ureido)quinolin-5-yl) oxy)picolinamide (**9k**)

White solid; yield 45.7%; mp 256–257 °C; ^{1}H NMR (400 MHz, DMSO-d_6) δ 12.35 (br. s, 1H), 10.49 (s, 1H), 8.82 (q, J = 4.4 Hz, 1H), 8.58 (d, J = 5.6 Hz, 1H), 8.44 (d, J = 8.4 Hz, 1H), 8.31 (d, J = 9.2 Hz, 1H), 8.26 (d, J = 7.6 Hz, 1H), 8.04 (d, J = 8.0 Hz, 1H), 7.92–7.87 (m, 2H), 7.81–7.74 (m, 2H), 7.65 (t, J = 7.6 Hz, 1H), 7.57 (t, J = 7.6 Hz, 1H), 7.46 (q, J = 4.0 Hz, 2H), 7.37 (dd, J = 6.0, 2.4 Hz, 1H), 7.27 (dd, J = 5.6, 2.4 Hz, 1H), 2.80 (d, J = 4.8 Hz, 3H); ^{13}C NMR (100 MHz, DMSO-d_6) δ 166.19, 164.14, 153.73, 153.14, 152.88, 151.15, 149.58, 146.90, 134.28, 134.21, 133.31, 131.60, 129.23, 126.84, 126.62, 126.50, 126.10, 124.15, 123.98, 121.43, 118.35, 117.87, 116.31, 115.09, 114.70, 109.61, 26.48; HRMS (ESI-TOF) *m/z* calcd for $C_{27}H_{21}N_5O_3Na$ $[M+Na]^+$: 486.1542, found: 486.1538.

4.11. Cancer cell line screening

Anticancer activity of the target compounds against human cancer cell lines was investigated using the MTT assay. HCT-116 (Human colorectal carcinoma), MCF-7 (breast cancer cells) and SK-BR3 (breast cancer cells) were supplied from the Korea Cell Line Bank (KCLB). All cell lines were grown in RPMI 1640/DMEM (Gibco BRL) supplemented with 10% (V/V) heat inactivated Fetal Bovine Serum (FBS) and maintained at 37 °C in a humidified atmosphere with 5% CO_2. The cells (5 × 104 cells/mL) were seeded into 96-well plate. Various concentrations of samples was added to each well in duplicate, then incubated at 37 °C with 5% CO_2 for two days such that time cells are in the exponential phase of growth at the time of compound addition. Add 15 μL of the Dye Solution (Promrga, Cell Titer 96) to each well. Incubate the plate at 37 °C for up to 4 h in a humidified, 5% CO_2 atmosphere. After incubation, add 100 μL of the Solubilization Solution/Stop Mix (Promrga, Cell Titer 96) to each well. Allow the plate to stand overnight in a sealed container with a humidified atmosphere at room temperature to completely solubilize the formazan crystals. The optical density was measured using a microplate reader (Versamax, Molecular Devices) with a 570 nm wavelength.

The cancer cell screening over full panel of 60 human cancer cell lines was applied at the National Cancer Institute (NCI), Bethesda, Maryland, USA [32] adopting the standard procedure [47].

4.12. In vitro kinase screening

Reaction Biology Corp. Kinase HotSpot^{SM} service [39] was used for screening of compounds **9b** and **9d**. Assay protocol: In a final reaction volume of 25 μL, kinase (5–10 mU) is incubated with 25 mM Tris pH 7.5, 0.02 mM EGTA, 0.66 mg/mL myelin basic protein, 10 μM magnesium acetate and [γ^{33}P-ATP] (specific activity approx. 500 cpm/pmol, concentration as required). The reaction is initiated by the addition of the Mg-ATP mix. After incubation for 40 min at room temperature, the reaction is stopped by the addition of 5 μL of a 3% phosphoric acid solution. 10 μL of the reaction is then spotted onto a P30 filtermat and washed three times for 5 min in 75 mM phosphoric acid and once in methanol prior to drying and scintillation counting.

4.13. Molecular docking

The docking model was carried out using the X-ray co-crystal structure of BRAF^{V600E}, in its DFG-out conformation, with sorafenib (PDB: 1UWJ) [45] and C-RAF homology model. For docking study with DFG-out conformation of C-RAF (amino acid code in Uniprot: P04049), the homology model of C-RAF copying with sorafenib was generated from a BRAF^{V600E} X-ray crystal structure using Modeller module implemented in Discovery Studio program. The homology model was selected with low PDF energy, and the proteins and ligands were respectively prepared using Protein-PrepareWizard and Ligprep module in Maestro 9.7 (Schrödinger, LLC, New York). After adding hydrogens, protein was neutralized and then optimized with energy minimization for only hydrogens. Ligand was prepared through protonation at pH 7.4 and energy minimization. Gold suite ver. 5.2 (CCDC, Cambridge, UK) with goldscore was employed to predict binding mode of ligand into BRAF^{V600E} and C-RAF. The pose with the highest gold score were selected as the best docking pose and used for analysis of binding mode.

4.14. Cell cycle analysis

The A498 renal carcinoma cell line was seeded in 6 cm dishes and incubated for overnight, followed by addition of the proper concentrations of the test compounds (based on their IC_{50} values) at the second day. The cells treated with the test compounds were incubated for 48 h. Untreated and treated cells were harvested, washed with phosphate-buffered saline (PBS), fixed in ice-cold 70% ethanol, and stained with propidium iodide. The cell cycle of the treated cells was analyzed by BD Calibur, and the data was analyzed by Modfit software.

Acknowledgments

This research was supported by the Korea Institute of Science and Technology (KIST) Institutional Program (2E25240 and 2E25473). We would like to express our sincere appreciation and gratitude to the National Cancer Institute (NCI, Bethesda, Maryland, USA) for carrying out the anticancer evaluation of the new compounds.

Appendix A. Supplementary data

Supplementary data related to this article can be found at http://dx.doi.org/10.1016/j.ejmech.2015.07.025.

References

[1] A. Jemal, R. Siegel, E. Ward, T. Murray, J. Xu, M.J. Thun, Cancer statistics, 2007, CA Cancer J. Clin. 57 (2007) 43–66.
[2] World Health Organization, Media Centre, Cancer, http://www.who.int/mediacentre/factsheets/fs297/en/ (retrieved on 22.05.15).
[3] M. Vanneman, G. Dranoff, Combining immunotherapy and targeted therapies in cancer treatment, Nat. Rev. Cancer 12 (2012) 237–251.
[4] A.K. El-Damasy, N.-C. Cho, S.B. Kang, A.N. Pae, G. Keum, ABL kinase inhibitory and antiproliferative activity of novel picolinamide based benzothiazoles, Bioorg. Med. Chem. Lett. 25 (2015) 2162–2168.
[5] B.S. Nam, H. Kim, C.H. Oh, S.H. Lee, S.J. Cho, T.B. Sim, J.M. Hah, D.J. Kim, J.H. Choi, K.H. Yoo, Aminoquinoline derivatives with antiproliferative activity against melanoma cell line, Bioorg. Med. Chem. Lett. 19 (2009) 3517–3520.
[6] H.F. Li, T. Lu, T. Zhu, Y.J. Jiang, S.S. Rao, L.Y. Hu, B.T. Xin, Y.D. Chen, Virtual screening for Raf-1 kinase inhibitors based on pharmacophore model of substituted ureas, Eur. J. Med. Chem. 44 (2009) 1240–1249.
[7] Q. Chao, K.G. Sprankle, R.M. Grotzfeld, A.G. Lai, T.A. Carter, A.M. Velasco, R.N. Gunawardane, M.D. Cramer, M.F. Gardner, J. James, P.P. Zarrinkar, H.K. Patel, S.S. Bhagwat, Identification of N-(5-tert-butyl-isoxazol-3-yl)-N′-{4-[7-(2-morpholin-4-yl-ethoxy)imidazo[2,1-b][1,3]benzothiazol-2-yl]phenyl} urea dihydrochloride (AC220), a uniquely potent, selective, and efficacious FMS-like tyrosine kinase-3 (FLT3) inhibitor, J. Med. Chem. 52 (2009) 7808–7816.
[8] A. Garofalo, A. Farce, S. Ravez, A. Lemoine, P. Six, P. Chavatte, L. Goossens, P. Depreux, Synthesis and structure-activity relationships of (aryloxy)quinazoline ureas as novel, potent, and selective vascular endothelial growth factor receptor-2 inhibitors, J. Med. Chem. 55 (2012) 1189–1204.
[9] W.S. Huang, C.A. Metcalf, R. Sundaramoorthi, Y. Wang, D. Zou, R.M. Thomas, X. Zhu, L. Cai, D. Wen, S. Liu, J. Romero, J. Qi, I. Chen, G. Banda, S.P. Lentini,

S. Das, Q. Xu, J. Keats, F. Wang, S. Wardwell, Y. Ning, J.T. Snodgrass, M.I. Broudy, K. Russian, T. Zhou, L. Commodore, N.I. Narasimhan, Q.K. Mohemmad, J. Iuliucci, V.M. Rivera, D.C. Dalgarno, T.K. Sawyer, T. Clackson, W.C. Shakespeare, Discovery of 3-[2-(imidazo[1,2-b]pyridazin-3-yl)ethynyl]-4-methyl-N-{4-[(4-methylpiperazin-1-yl)methyl]-3-(trifluoromethyl)phenyl}benzamide (AP24534), a potent, orally active pan-inhibitor of breakpoint cluster region-abelson (BCR-ABL) kinase including the T315I gatekeeper mutant, J. Med. Chem. 53 (2010) 4701–4719.

[10] T.B. Lowinger, B. Riedl, J. Dumas, R.A. Smith, Design and discovery of small molecules targeting Raf-1 kinase, Curr. Pharm. Des. 8 (2002) 2269–2278.

[11] D. Strumberg, Preclinical and clinical development of the oral multikinase inhibitor sorafenib in cancer treatment, Drugs Today 41 (2005) 773–784.

[12] L. Liu, Y. Cao, C. Chen, X. Zhang, A. McNabola, D. Wilkie, S. Wilhelm, M. Lynch, C. Carter, Sorafenib blocks the RAF/MEK/ERK pathway, inhibits tumor angiogenesis, and induces tumor cell apoptosis in hepatocellular carcinoma model PLC/PRF/5, Cancer Res. 66 (2006) 11851–11858.

[13] S.M. Wilhelm, L. Adnane, P. Newell, A. Villanueva, J.M. Llovet, M. Lynch, Preclinical overview of sorafenib, a multikinase inhibitor that targets both Raf and VEGF and PDGF receptor tyrosine kinase signaling, Mol. Cancer Ther. 7 (2008) 3129–3140.

[14] S.M. Wilhelm, L. Adnane, P. Newell, A. Villanueva, J.M. Llovet, M. Lynch, Preclinical overview of sorafenib, a multikinase inhibitor that targets both Raf and VEGF and PDGF receptor tyrosine kinase signaling, Mol. Cancer Ther. 7 (2008) 3129–3140.

[15] J.M. Llovet, S. Ricci, V. Mazzaferro, P. Hilgard, E. Gane, J.F. Blanc, A.C. de Oliveira, A. Santoro, J.L. Raoul, A. Forner, M. Schwartz, C. Porta, S. Zeuzem, L. Bolondi, T.F. Greten, P.R. Galle, J.F. Seitz, I. Borbath, D. Haussinger, T. Giannaris, M. Shan, M. Moscovici, D. Voliotis, J. Bruix, Sorafenib in advanced hepatocellular carcinoma, New Engl. J. Med. 359 (2008) 378–390.

[16] L. Rimassa, A. Santoro, Sorafenib therapy in advanced hepatocellular carcinoma: the SHARP trial, Expert Rev. Anticancer Ther. 9 (2009) 739–745.

[17] B. Escudier, M.D. Michaelson, R.J. Motzer, T.E. Hutson, J.I. Clark, H.Y. Lim, E. Porfiri, P. Zalewski, G. Kannourakis, M. Staehler, J. Tarazi, B. Rosbrook, L. Cisar, S. Hariharan, S. Kim, B.I. Rini, Axitinib versus sorafenib in advanced renal cell carcinoma: subanalyses by prior therapy from a randomised phase III trial, Br. J. Cancer 110 (2014) 2821–2828.

[18] Clinical Trials of Sorafenib, http://clinicaltrial.gov/ct2/results?term=sorafenib&Search=Search (retrieved on 22.05.15).

[19] S. Ramurthy, S. Subramanian, M. Aikawa, P. Amiri, A. Costales, J. Dove, S. Fong, J.M. Jansen, B. Levine, S. Ma, C.M. McBride, J. Michaelian, T. Pick, D.J. Poon, S. Girish, C.M. Shafer, D. Stuart, L. Sung, P.A. Renhowe, Design and synthesis of orally bioavailable benzimidazoles as Raf kinase inhibitors, J. Med. Chem. 51 (2008) 7049–7052.

[20] T. Eisen, T. Ahmad, K.T. Flaherty, M. Gore, S. Kaye, R. Marais, I. Gibbens, S. Hackett, M. James, L.M. Schuchter, K.L. Nathanson, C. Xia, R. Simantov, B. Schwartz, M. Poulin-Costello, P.J. O'Dwyer, M.J. Ratain, Sorafenib in advanced melanoma: a phase II randomised discontinuation trial analysis, Br. J. Cancer 95 (2006) 581–586.

[21] F.A.B. Schutz, Y. Je, T.K. Choueiri, Hematologic toxicities in cancer patients treated with the multi-tyrosine kinase sorafenib: a meta-analysis of clinical trials, Crit. Rev. Oncol. Hematol. 80 (2011) 291–300.

[22] T. Otsuka, Y. Eguchi, S. Kawazoe, K. Yanagita, K. Ario, K. Kitahara, H. Kawasoe, H. Kato, T. Mizuta, Skin toxicities and survival in advanced hepatocellular carcinoma patients treated with sorafenib, Hepatol. Res. 42 (2012) 879–886.

[23] O. Mir, R. Coriat, B. Blanchet, J.P. Durand, P. Boudou-Rouquette, J. Michels, S. Ropert, M. Vidal, S. Pol, S. Chaussade, F. Goldwasser, Sarcopenia predicts early dose-limiting toxicities and pharmacokinetics of sorafenib in patients with hepatocellular carcinoma, PLoS One 7 (2012) e37563.

[24] Y. Dai, K. Hartandi, Z. Ji, A.A. Ahmed, D.H. Albert, J.L. Bauch, J.J. Bouska, P.F. Bousquet, G.A. Cunha, K.B. Glaser, C.M. Harris, D. Hickman, J. Guo, J. Li, P.A. Marcotte, K.C. Marsh, M.D. Moskey, R.L. Martin, A.M. Olson, D.J. Osterling, L.J. Pease, N.B. Soni, K.D. Stewart, V.S. Stoll, P. Tapang, D.R. Reuter, S.K. Davidsen, M.R. Michaelides, Discovery of N-(4-(3-amino-1H-indazol-4-yl) phenyl)-N′-(2-fluoro-5-methylphenyl)urea (ABT-869), a 3-aminoindazole-based orally active multitargeted receptor tyrosine kinase inhibitor, J. Med. Chem. 50 (2007) 1584–1597.

[25] M.H. Potashman, J. Bready, A. Coxon, T.M. DeMelfi, L. DiPietro, N. Doerr, D. Elbaum, J. Estrada, P. Gallan, J. Germain, Y. Gu, J.C. Harmange, S.A. Kaufman, R. Kendall, J.L. Kim, G.N. Kumar, A.M. Long, S. Neervannan, V.F. Patel, A. Polverino, P. Rose, S. van der Plas, D. Whittington, R. Zanon, H. Zhao, Design, synthesis, and evaluation of orally active benzimidazoles and benzoxazoles as vascular endothelial growth factor-2 receptor tyrosine kinase inhibitors, J. Med. Chem. 50 (2007) 4351–4373.

[26] D. Menard, I. Niculescu-Duvaz, H.P. Dijkstra, D. Niculescu-Duvaz, B.M.J.M. Suijkerbuijk, A. Zambon, A. Nourry, E. Roman, L. Davies, H.A. Marine, F. Friedlos, R. Kirk, S. Whittaker, A. Gill, R.D. Taylor, R. Marais, C.J. Springer, Novel potent BRAF inhibitors: toward 1 nM compounds through optimization of the central phenyl ring, J. Med. Chem. 52 (2009) 3881–3891.

[27] M.H. Jung, H. Kim, W.K. Choi, M.I. El-Gamal, J.H. Park, K.H. Yoo, T.B. Sim, S.H. Lee, D. Baek, J.M. Hah, J.H. Cho, C.H. Oh, Synthesis of pyrrolo[2,3-d]pyrimidine derivatives and their antiproliferative activity against melanoma cell line, Bioorg. Med. Chem. Lett. 19 (2009) 6538–6543.

[28] H.J. Kim, H.J. Cho, H. Kim, M.I. El-Gamal, C.H. Oh, S.H. Lee, T. Sim, J.M. Hah, K.H. Yoo, New diarylureas and diarylamides possessing acet(benz)amidophenyl scaffold: design, synthesis, and antiproliferative activity against melanoma cell line, Bioorg. Med. Chem. Lett. 22 (2012) 3269–3273.

[29] I. Niculescu-Duvaz, A. Zambon, D. Niculescu-Duvaz, S. Whittaker, R. Marais, C.J. Springer, Preparation of substituted aryl-quinolyl ureas and amides and their use, PCT Pat. Appl. WO 2009130487, October 29, 2009.

[30] M.H. Son, J.Y. Kim, E.J. Lim, D.J. Baek, K. Choi, J.K. Lee, A.N. Pae, S.J. Min, Y.S. Cho, Synthesis and biological evaluation of 2-(arylethynyl)quinoline derivatives as mGluR5 antagonists for the treatment of neuropathic pain, Bioorg. Med. Chem. Lett. 23 (2013) 1472–1476.

[31] J.Y. Kim, M.H. Son, K. Choi, D.J. Baek, M.K. Ko, E.J. Lim, A.N. Pae, G. Keum, J.K. Lee, Y.S. Cho, H. Choo, Y.W. Lee, B.S. Moon, B.C. Lee, H.Y. Lee, S.J. Min, Synthesis and in vivo evaluation of 5-methoxy-2-(phenylethynyl)quinoline (MPEQ) and [C-11]MPEQ targeting metabotropic glutamate receptor 5 (mGluR5), Bull. Korean Chem. Soc. 35 (2014) 2304–2310.

[32] NCI Website: www.dtp.nci.nih.gov.

[33] DTP Data Search: http://dtp.nci.nih.gov/dtpstandard/dwindex/index.jsp (retrieved on 22.05.15).

[34] H.J. Bohm, D. Banner, S. Bendels, M. Kansy, B. Kuhn, K. Muller, U. Obst-Sander, M. Stahl, Fluorine in medicinal chemistry, Chembiochem 5 (2004) 637–643.

[35] U.L.R. Maggiore, M.V. Menada, P.L. Venturini, S. Ferrero, Sorafenib for ovarian cancer, Expert Opin. Investig. Drug 22 (2013) 1049–1062.

[36] D. Matei, M.W. Sill, H.A. Lankes, K. DeGeest, R.E. Bristow, D. Mutch, S.D. Yamada, D. Cohn, V. Calvert, J. Farley, E.F. Petricoin, M.J. Birrer, Activity of sorafenib in recurrent ovarian cancer and primary peritoneal carcinomatosis: a Gynecologic Oncology Group trial, J. Clin. Oncol. 29 (2011) 69–75.

[37] J. Zhang, K.A. Gold, E. Kim, Sorafenib in non-small cell lung cancer, Expert Opin. Investig. Drug 21 (2012) 1417–1426.

[38] W.L. Wang, Z.H. Tang, T.T. Xie, B.K. Xiao, X.Y. Zhang, D.H. Guo, D.X. Wang, F. Pei, H.Y. Si, M. Zhu, Efficacy and safety of sorafenib for advanced non-small cell lung cancer: a meta-analysis of randomized controlled trials, Asian Pac. J. Cancer Prev. 15 (2014) 5691–5696.

[39] Reaction Biology Corporation Web Site. Available from: www.reactionbiology.com.

[40] H. Hao, V.M. Muniz-Medina, H. Mehta, N.E. Thomas, V. Khazak, C.J. Der, J.M. Shields, Context-dependent roles of mutant B-Raf signaling in melanoma and colorectal carcinoma cell growth, Mol. Cancer Ther. 6 (2007) 2220–2229.

[41] H. Tanami, I. Imoto, A. Hirasawa, Y. Yuki, I. Sonoda, J. Inoue, K. Yasui, A. Misawa-Furihata, Y. Kawakami, J. Inazawa, Involvement of overexpressed wild-type BRAF in the growth of malignant melanoma cell lines, Oncogene 23 (2004) 8796–8804.

[42] B. Zheng, J.H. Jeong, J.M. Asara, Y.-Y. Yuan, S.R. Granter, L. Chin, L.C. Cantley, Oncogenic B-RAF negatively regulates the tumor suppressor LKB1 to promote melanoma cell proliferation, Mol. Cell 33 (2009) 237–247.

[43] H. Oka, Y. Chatani, R. Hoshino, O. Ogawa, Y. Kakehi, T. Terachi, Y. Okada, M. Kawaichi, M. Kohno, O. Yoshida, Constitutive activation of mitogen-activated protein (MAP) kinases in human renal cell carcinoma, Cancer Res. 55 (1995) 4182–4187.

[44] F. McPhillips, P. Mullen, B.P. Monia, A.A. Ritchie, F.A. Dorr, J.F. Smyth, S.P. Langdon, Association of c-Raf expression with survival and its targeting with antisense oligonucleotides in ovarian cancer, Br. J. Cancer 85 (2001) 1753–1758.

[45] P.T.C. Wan, M.J. Garnett, S.M. Roe, S. Lee, D. Niculescu-Duvaz, V.M. Good, C.M. Jones, C.J. Marshall, C.J. Springer, D. Barford, R. Marais, C.G. Project, Mechanism of activation of the RAF-ERK signaling pathway by oncogenic mutations of B-RAF, Cell 116 (2004) 855–867.

[46] http://www.organic-chemistry.org/prog/peo.

[47] DTP Human Tumor Cell Line Screen Process: http://www.dtp.nci.nih.gov/branches/btb/ivclsp.html (retrieved on 22.05.15).